MEMO 2-5-59E

NASA

MEMORANDUM

AN EQUATION FOR THE MEAN VELOCITY DISTRIBUTION OF BOUNDARY LAYERS

By V. A. Sandborn

Lewis Research Center
Cleveland, Ohio

NATIONAL AERONAUTICS AND SPACE ADMINISTRATION
WASHINGTON
February 1959

NATIONAL AERONAUTICS AND SPACE ADMINISTRATION

MEMORANDUM 2-5-59E

AN EQUATION FOR THE MEAN VELOCITY DISTRIBUTION OF BOUNDARY LAYERS

By V. A. Sandborn

SUMMARY

A general relation, empirical in origin, for the mean velocity distribution of both laminar and turbulent boundary layers is proposed. The equation, in general, accurately describes the profiles in both laminar and turbulent flows. The calculation of profiles is based on a prior knowledge of momentum, displacement, and boundary-layer thickness together with free-stream conditions. The form for turbulent layers agrees with the present concepts of similarity of the outer layer. For the inner region or turbulent boundary layers the present relation agrees very closely with experimental measurements even in cases where the logarithmic law of the wall is inadequate.

A unique relation between profile form factors and the ratio of displacement thickness to boundary-layer thickness is obtained for turbulent separation. A similar criterion is also obtained for laminar separation. These relations are demonstrated to serve as an accurate criterion for identifying separation in known profiles.

INTRODUCTION

Empirical methods exist for predicting such important quantities as skin friction and heat transfer in boundary layers. From the standpoint of basic mechanics, however, there is still much to be learned about boundary layers. Of the many approximate methods of dealing with boundary layers, no one solution is general enough to completely describe both the laminar and turbulent boundary layers.

It is reasonable to suspect that a general solution of the equations of motion would include both laminar and turbulent flows as special cases. Indeed, reference 1 has demonstrated that it is possible to construct a relation for the mean velocity of channel flow which is applicable for either laminar or turbulent flow. Recently, evidence was presented (ref. 2) suggesting a possible relation of the known laminar boundary solutions to the measured outer region of turbulent boundary layers. Thus, it appears of interest to investigate the possibility of finding one relation to represent the complete velocity distribution of boundary layers.

While of academic interest, a general relation for the velocity distribution, though expected, would not be too useful as an engineering tool, since it would be far too complex to be directly applicable. Study of a general relation could serve as a guide to the development of consistent flow models of special cases, such as turbulent separation and laminar-turbulent transition. It would further be of great value in the analysis of experimental data. As an ultimate objective, this general relation could point the way toward the theoretical solution of the boundary-layer equations.

The present analysis treats one possible empirical relation, which appears to represent the velocity distributions of either laminar or turbulent boundary layers in incompressible fluids. The relation is a modification of the relation employed in reference 1 to represent the velocity distribution in the channel. An attempt to apply the relation of reference 1 directly to boundary-layer flow was made in reference 3. The results of reference 3, while encouraging, did not give as accurate a representation of turbulent boundary-layer velocity profiles as would be desirable. Since the presentation of reference 3, it was found that another step in the generalization of the relation could be made without introducing any further complication. The relation also works in the laminar region of the boundary layer. The present relation is of greater value in the analysis of experimental data and the study of the structure of the turbulent boundary layer, rather than in the engineering prediction of boundary-layer development.

BASIC EQUATION

The present relation for the mean velocity distribution is empirical. Although it is suggested in what follows that there is certain justification for the relation, its proof can only be judged by how well the relation fits the known velocity distributions. As a logical first step in the development of the relation, current knowledge about boundary layers is reviewed. The object of such a review is to form a consistent model for the flow in the boundary layer.

Description of the Boundary Layer

The model for the turbulent boundary layer must conform to certain established facts. (The primary concern is the establishment of a mathematical model for the layer.) In particular, the layer can be divided into roughly two regions where the flow characteristics are different. The regions are: (1) The outer (major) portion of the boundary layer where the transfer of momentum and energy are largely accomplished by the turbulent fluctuations. (2) The region very near the wall where the effects of viscosity, as well as the turbulent fluctuations, must be important.

The outer region of the turbulent boundary layer was extensively studied in reference 2. It was demonstrated that this outer-region velocity distribution is similar to a laminar velocity distribution. Briefly, the picture of the turbulent velocity profiles proposed in reference 2 is a laminar profile of high viscosity with a very thin sublayer of a different fluid with much lower viscosity. An analysis presented in reference 1 for the turbulent velocity distribution in a channel also implies this similarity to a laminar flow in that the velocity profile in the outer region of fully developed turbulent channel flow is approximately the same as the laminar distribution.

In an earlier investigation (ref. 4) it was observed that similar velocity distributions in this outer region could be obtained by proper selection of the static-pressure distribution. Reference 4 demonstrated that the distribution of velocity in the outer region was nearly independent of the inner region, and that such parameters as momentum thickness and displacement thickness depended only on the distribution in the outer region. In a more recent work (ref. 2) proof was given to show that the similarity was not exact, but that it was satisfied within experimental accuracy.

The flow mechanism near the wall will be more complex than that in the outer region, in that both viscosity and turbulent transport of momentum and energy are important. The present analysis takes issue with the mixing length and laminar sublayer model generally assumed for this inner region. The concept of an eddy viscosity implied by the mixing length theory may be retained for the present analysis (application of the eddy viscosity for pipe flow with the equivalent equation as studied herein was made in ref. 5); however, the logarithmic velocity distribution could not be justified. In recent years there has been strong support for an assumption that the logarithmic-type distribution, obtained from mixing length theory, is a universal distribution for all turbulent boundary-layer flow. However, it is suspected that the similarity observed for this inner region is only approximate, as in the case of the outer region. If the concept of a similarity of the outer region is modified (demonstrated in ref. 6), the logarithmic distribution for the inner region is only a particular solution of a more general power law relation. (The work of ref. 6 was done unaware of (or before) that completed in ref. 2. In ref. 6 the assumptions of modified similarity were based on suggestions made by A. A. Townsend.) It is important to note that while the data of reference 7 are cited extensively to justify the logarithmic distribution in the different pressure gradient flows, they demonstrate that a power-law distribution fits the data (see fig. 1, ref. 7). The versatile skin-friction equation derived in reference 7 depends on the existence of a power law distribution for the velocity near the wall.

One concept that is not included in the present model for the turbulent boundary layer is the "laminar sublayer." (Of course, a question of

definition may arise here since laminar sublayer may be the term applied to the complete inner region. However, the word "laminar", flow in layers, is out of place in such a definition.) While viscosity will dissipate a great deal of turbulent energy in the region adjacent to the wall, no justification can be found for the assumption that all the turbulent energy must be dissipated before the wall is reached.

For the present model of flow in the inner region of the turbulent boundary layer, it is assumed that the influences of wall and viscosity are evidenced by the orientation of the direction of the axis of rotation of eddies, and by the dissipation of turbulent energy. It has been shown (ref. 8, see fig. 25) that the principal axis of the turbulent stress tensor tends toward a direction that is parallel to the wall as the wall is approached. This approach is believed to show that the eddies become parallel to the wall in this region. Thus, the "virtual viscosity" decreases as the wall is approached (reaching the molecular value at the wall) because of the eddy motion becoming parallel to the wall. The model is crude in that the eddies are far from two-dimensional, so that the concept of a principal axis has statistical meaning only. This model does not consider the possibility of a production of turbulent energy, as well as a dissipation, in this inner region.

In summary, the present model for turbulent boundary layer indicates an outer region of homogeneous turbulence (as far as transport properties are concerned), wherein the turbulence can be replaced by a constant eddy viscosity. Similar velocity profiles are possible in this outer region to a reasonable degree of approximation. In the inner region, which is only a very small part of the complete layer, both turbulent and molecular transport properties exist. The turbulent transport in the inner region decreases as the wall is approached, partly because of the turbulent eddies laying over parallel to the wall, and also because of viscosity dissipating the turbulent energy. While the trend in the inner region is toward a laminar flow, no completely laminar region exists. The velocity distribution in the inner region is more likely to be a power law relation rather than a logarithmic relation.

Development of the Empirical Mean Velocity Profile Equation

The present model no doubt will be improved as the understanding of turbulence becomes more complete. For the present it can give some justification for the boundary-layer velocity equation employed.

The form of the equation is suggested in reference 1. Reference 1 further demonstrates how the relation not only represents the velocity distribution, but also predicts the measured turbulent shear-stress distribution.

The fact that the flow in boundary layers is similar to that in channels has long been realized. Thus, an attempt was made to apply the relation of reference 1 to the turbulent boundary layer (see ref. 3). The relation proved only approximately correct, as might have been expected, since the boundary layer has more freedom of motion than that of fully developed channel flow. However, the relations suggested from the analysis of reference 3 have led to some extensions, which are incorporated in the present analysis. In reference 3 the relation from reference 1 was employed directly as

$$\frac{U}{U_1} = A + B\left(1 - \frac{y}{\delta}\right)^2 + C\left(1 - \frac{y}{\delta}\right)^{2n} \tag{1}$$

where A, B, and C were determined from boundary conditions. (Symbols are defined in appendix A.) An important observation of reference 3 was that the square power term contributes greatly in the outer region of the layer; both power terms contribute in the inner region. For turbulent channel flow the square term is necessary so that the equation can be reduced to the exact laminar velocity distribution, and in line with the results of reference 2, the outer region of turbulent channel flow must vary like the laminar velocity distribution. Thus, for channel flow equation (1) corresponds to the model of the outer region of the flow. However, for laminar boundary-layer flow the use of a square power would not be expected to be exact. A generalization of equation (1) is therefore necessary if accurate results are to be obtained for a boundary layer. As the next logical step in equation (1), the square power term is replaced by an arbitrary power m. The power 2n is retained as such, so that the present notation remains the same as references 1 and 3. It is, of course, obvious that m and 2n are interchangeable without altering the basic equation. However, for the present analysis the boundary conditions are employed so that m will correspond to the square term for the proper profile. In other words, m will correspond to the power for a laminar velocity distribution.

The present analysis starts with the following equation:

$$\frac{U}{U_1} = A + B\left(1 - \frac{y}{\delta}\right)^m + C\left(1 - \frac{y}{\delta}\right)^{2n} \tag{2}$$

A, B, and C are evaluated from the following boundary conditions, which are valid for both laminar and turbulent boundary layers when

$$\left.\begin{array}{l} y = 0 \begin{cases} U = 0 \\ \dfrac{\partial U}{\partial y} = \dfrac{\tau_w}{\mu} \end{cases} \\ y = \delta \begin{cases} U = U_1 \\ \dfrac{\partial U}{\partial y} = 0 \end{cases} \end{array}\right\} \tag{3}$$

The values of A, B, and C are

$$\left.\begin{array}{l} A = 1 \\ B = \dfrac{2(s - n)}{2n - m} \equiv \zeta \\ C = -\dfrac{2s - m}{2n - m} = -(1 + \zeta) \end{array}\right\} \tag{4}$$

where s is a fundamental wall shear-stress parameter defined as

$$s = \frac{\delta \tau_w}{2U_1 \mu}$$

For channel flow, with δ equal to the channel half-width, s is a ratio of the wall shear stress τ_w to the corresponding laminar (same maximum velocity U_1) wall shear stress $2U_1\mu/\delta$. The parameter ζ, as noted in equation (4), is used for the value of the particular grouping of s, m, and 2n encountered. Equation (2) is rewritten as

$$\frac{U}{U_1} = 1 + \zeta\left(1 - \frac{y}{\delta}\right)^m - (1 + \zeta)\left(1 - \frac{y}{\delta}\right)^{2n} \tag{5}$$

Equation (5) is a general relation for the mean velocity distribution in boundary layers, or for any shear flow for which the boundary conditions (eq. (3)) are valid. There are four constants, δ, m, 2n, and s, which must be known to completely specify the profile.

General limits on the magnitude of the constants are as yet unknown. The boundary conditions (eq. (3)) require positive values of m and 2n. The values of m and 2n are not limited to whole numbers in order to obtain accurate distributions; therefore, the high-order velocity derivatives at the outer edge of the boundary layer ($y = \delta$) may not be finite. (The failure to match high-order velocity derivatives is a disadvantage of most empirical relations for the velocity distribution.)

However, the high-order velocity derivatives do not generally enter into boundary-layer calculations. A distribution can be calculated for both positive and negative (reverse flow) values of the skin-friction parameter s (ref. 3, see fig. 1(c)). The special cases of the constants, $2s = 2n = m$ and $m = 2n$, will be considered in the section on laminar flow. The case of $2n = \infty$ will prove of value in the separation region.

The present constants, ζ, m, and 2n are related to the familiar boundary-layer parameters, displacement and momentum thickness, by the following equations

$$\frac{\delta^*}{\delta} = -\frac{\zeta}{m+1} + \frac{1+\zeta}{2n+1} \tag{6}$$

and

$$\frac{\theta}{\delta} = -\frac{\zeta}{m+1} - \frac{\zeta^2}{2m+1} + (1+\zeta)\left[\frac{2\zeta}{2n+m+1} + \frac{1}{2n+1} - \frac{(1+\zeta)}{4n+1}\right] \tag{7}$$

This report now discusses the adequacy with which equation (5) represents both laminar and turbulent velocity distributions.

THE TURBULENT BOUNDARY LAYER

Turbulent flow is considered first since it is the more complex case of boundary-layer flow. The present analysis demonstrates how equation (5) will fit measured turbulent boundary-layer profiles. The ultimate engineering objective would, of course, be that equation (5) may be used to predict the development of turbulent boundary layers. However, the present analysis cannot proceed beyond the prediction of the velocity distribution, once the values of the necessary constants are determined from other sources. To someone unfamiliar with the literature on turbulence the fitting of an analytical expression to an already measured profile may not appear to be of much value. However, the present state of knowledge of turbulent boundary-layer flow is incomplete, therefore, the mere fitting of experimental data is still a major problem. Apparently, the only method found in the literature for fitting a complete curve through the turbulent mean velocity data (with exception of ref. 3) is that developed in reference 9. Tables were compiled in reference 9 (from experimental data), which when used with experimental values of skin friction and various coefficients give reasonable velocity distributions for the turbulent boundary layer. The results are based on the hypothesis that similarity exists for both the outer and inner regions of the boundary layer. The present general relation does not require the existence of similarity, but similarity will prove useful in the application of the relation.

Comparison with Measured Velocity Distributions

Direct evaluating of equation (5) for any particular measured profile is a problem of determining m and 2n, since δ and s can be found from direct measurements. For the present determination, m and 2n are expressed in terms of δ^* and θ, since these values can readily be obtained from the measured data. Use of equations (6) and (7) (with knowledge of δ and s) directly to evaluate m and 2n in terms of δ^* and θ is quite tedious; however, it will be demonstrated later that it is possible to make an approximation which greatly simplifies the calculations. An outline of the method of calculating a profile is given in appendix B.

Figure 1 compares actual measured profiles with the predicted distributions of equation (5). The value of δ for these profiles was arbitrarily taken as the point where the free-stream velocity appeared to be reached. The proper value of δ, independent of an arbitrary choice, could be obtained from measurements of the intermittancy of turbulence (see ref. 10); however, intermittency measurements are not available for the profiles presented in figure 1.

For figures 1(a) and (b) the values of wall shear stress, necessary in determining s, were obtained from local heat-transfer measurements (see ref. 10). For figure 1(c) the skin-friction value was obtained from the relation developed in reference 7. Figure 1(d) shows the separation profile measured in reference 11; as will be shown later no skin-friction value was required. The heat-transfer method was also employed in reference 7 in order to evaluate the skin friction of figure 1(e). Figure 1(f) shows a separation profile in which an uncertainty in skin friction exists. In order to fit the profile (fig. 1(f)) it was assumed that 2n had increased to such a large value that it might be taken as infinite; in this case no value of s is required. This conclusion will be covered more fully in the section Separation Region.

In most cases the fit of equation (5) to the measured data is quite good. Note that on figure 1(a) a curve predicted by the method outlined in reference 3 is also included to show the improvement of the present approach. It would have been surprising had the predictions of equation (5) not fitted the measurements, since the relation was forced to meet all boundary conditions including the shear at the wall plus two integral values. The fitting of equation (5) to the data is, of course, sensitive to the values of δ, δ^*, and θ used. A slight change in any one of the parameters may alter the fit of equation (5). For the thicker boundary layers, such as those of figures 1(a) to (d) the parameters are known quite accurately, and no great question arises in their determination. However, for the profiles, such as the data of figure 1(e), which must be taken from small plots, the accuracy of evaluating the parameters is limited. For the two profiles of figure 1(e), δ was chosen in each case

as the last plotted point of the data of reference 7. In each case it appears that a somewhat better fit could have been obtained if a slightly different value of δ were used.

A region may be noted in figures 1(c) and (d) for small y/δ, where the predictions appear to be low as compared with the measured points. Since these data (figs. 1(c) and (d)) are for profiles in and near the separation region, some question of the experimental accuracy exists. However, it is suspected that this deviation may indicate a fundamental difference between the predictions of equation (5) and actual flow conditions. As noted in the discussion of the flow model for turbulent boundary layers, there is no provision made in the present analysis to account for any subregions of abnormally high turbulence. Reference 12 reported evidence which suggests such local maximums of turbulent energy in the separation region. Recent unpublished hot-wire measurements (recorded by V. A. Sandborn) also appears to confirm the findings of reference 12 for the region near separation.

Similarity of the Outer Region of the Turbulent Boundary Layer

As noted previously the concept of similarity has been employed to study both the inner and outer regions of the boundary layer. It is instructive to examine the present velocity profile equation from the standpoint of similarity, since similarity can be shown to give an approximate method of evaluating the parameter m. In order to develop the concept of similarity in the outer region, the ideas illustrated in references 2 and 4 are reviewed briefly.

Reference 4 demonstrates experimentally that for particular pressure distributions, obtained by trial and error, a turbulent boundary-layer flow can be established in which all the velocity profiles for the outer region are identical when plotted as $\frac{U - U_1}{U_\tau}$ against $\frac{y}{\delta}$. Such flows were termed equilibrium flows and will, henceforth, be referred to as such. Two parameters

$$\Delta = \int_0^\infty \frac{U_1 - U}{U_\tau} \, dy \tag{8}$$

and

$$G = \frac{\int_0^\infty \left(\frac{U_1 - U}{U_\tau}\right)^2 dy}{\Delta} \tag{9}$$

were employed to specify each particular equilibrium flow. Obviously, if $\frac{U - U_1}{U_\tau}$ is a unique function of $\frac{y}{\delta}$, as required for an equilibrium flow, then Δ/δ and G are unique constants for the same equilibrium flow. It should be kept in mind that the profiles only approach identical profiles in the outer region of the layer, so Δ/δ and G will vary slightly from one profile to another even for the same equilibrium flow (since U_1/U_τ is not necessarily constant in equilibrium flows). However, the inner region where the similarity is not valid is so small compared with the outer region that the experimental value of the integrals (8) and (9) is unaffected by the deviation.

The parameters, displacement and momentum thickness, are related to Δ and G, respectively, through the skin friction as

$$\delta^* = \sqrt{\frac{C_f}{2}}\,\Delta \tag{10}$$

and

$$\theta = \sqrt{\frac{C_f}{2}}\left(1 - G\sqrt{\frac{C_f}{2}}\right)\Delta \tag{11}$$

Equations (10) and (11) may be combined and rewritten as follows

$$\frac{\theta}{\delta} = \frac{\delta^*}{\delta} - \left(\frac{G}{\Delta/\delta}\right)\left(\frac{\delta^*}{\delta}\right)^2 \tag{12}$$

Thus, for an equilibrium flow $\left(\frac{G}{\Delta/\delta}\right)$ is a constant, and a unique relation between θ/δ and δ^*/δ is predicted.

Equation (12) is the clue, which brought about the present generalization of the equation of reference 3. In reference 3 it was noted that by neglecting terms of order $1/2n$ in the expressions for momentum and displacement thickness (corresponding to equations (6) and (7) of the present analysis) an equation of the form of equation (12) was obtained. (It is now evident that ref. 3 was dealing with the particular equation for the equilibrium flow defined by $\left(\frac{G}{\Delta/\delta}\right) = \frac{9}{5}$.) The present analysis gives the relation

$$\frac{\theta}{\delta} = \frac{\delta^*}{\delta} - \frac{(m+1)^2}{(2m+1)}\left(\frac{\delta^*}{\delta}\right)^2 \tag{13}$$

when terms of order $1/2n$ are dropped from equations (6) and (7), and the two equations are combined. (As can be seen in fig. 1, $2n$ is always an order of magnitude larger than m.) It follows that for equations (12) and (13) to be equivalent, m must be a constant for each particular set of equilibrium flows. The relation between m and $\left(\frac{G}{\Delta/\delta}\right)$ is

$$m = \left(\frac{G}{\Delta/\delta}\right) - 1 + \sqrt{\left(\frac{G}{\Delta/\delta}\right)\left[\left(\frac{G}{\Delta/\delta}\right) - 1\right]} \tag{14}$$

The plus sign is used for the square root term in order to ensure an m value always positive and greater than one, as is required in the velocity equation.

The agreement with the similarity assumptions of reference 4 can be demonstrated by rewriting equation (5) if the $2n$ power term is dropped completely. In the parameters used for similar profiles the relation becomes

$$\frac{U_1 - U}{U_\tau} = \frac{\Delta}{\delta}(m + 1)\left(1 - \frac{y}{\delta}\right)^m \tag{15}$$

which requires at $y = 0$ $(U = 0)$

$$\frac{U_1}{U_\tau} = \frac{\Delta}{\delta}(m + 1) = \text{constant} \tag{16}$$

Equation (15) can be compared with the results of reference 4 by setting $m = 1.8$ for constant pressure flow (as computed from the values of $\Delta/\delta = 3.6$ and $G = 6.1$ given in ref. 4). In particular, reference 2 fits the known laminar profiles to the outer region of measured turbulent profiles. Figure 2(a) compares equation (15) for the flat-plate case with a curve of the family of Blasius profiles. While the agreement is certainly good, it is suspected that it might even be better than shown, since reference 4 notes: "In plotting these curves a small correction was made in the constant 3.6 to account for the fact that the laminar profiles are not expected to represent the turbulent profiles in the inner 10 to 20 percent of the layer." A slight change in the constant 3.6 could account for the disagreement of the present relation and that given in reference 4.

Figure 2(b) shows a comparison of equation (15) evaluated from the constants for pressure distributions 1 and 2 (ref. 4). A representative laminar profile reported in reference 2 is also shown for each profile. The fit of the present profile could be improved by a slight adjustment in Δ/δ.

A further comparison of the flat-plate profile with an experimental measurement is made in figure 3 in order to determine an accurate value for m. The comparison with the analysis of reference 2 shows that for optimum fitting of the present relation a slight adjustment in the constants is required. The dashed curve of figure 3 demonstrates the improvement of fit when the value of Δ/δ is taken as 3.5 instead of 3.6. The value of G was not changed.

The results of the present analysis of similarity profiles need not be limited to only equilibrium flows. Equation (13) is expected to apply for any turbulent flow in which $2n >> m$. It is observed experimentally that the condition $2n >> m$ becomes progressively better the farther the flow is from the transition region. Obviously, the region of application of the approximation is governed by the concept that the thickness of the sublayer decreases as the Reynolds number based on distance downstream increases.

The present analysis may be employed to indicate the approach of a boundary layer to an equilibrium flow. The data of reference 13 shows the severe case of a zero pressure gradient boundary layer disturbed by a rod. Figure 4 shows three profiles measured at different x-distances downstream of a 0.24-inch-diameter cylindrical rod in contact with the wall. The dashed curves on figure 4 are the zero pressure gradient equilibrium profiles obtained from equation (15) with $m = 1.9$. For figure 4(c) the profile is approaching closely the equilibrium profile predicted for the outer region.

The solid curves of figure 4 were obtained by using equation (13) to evaluate m and then using equation (6) in the approximate form

$$\zeta \approx -(m + 1)\frac{\delta^*}{\delta} \tag{17}$$

to evaluate ζ. The rod represents the case where turbulence is produced excessively at a location within the boundary, thus, the general equation is not a good fit of the measurements.

Similarity of the Inner Region of the Turbulent Boundary Layer

The concepts of similarity of the inner region stems from considerations of mixing length and dimensional analysis. The variables U/U_τ and yU_τ/ν have been accepted as the similarity coordinates, with large volumes of data supporting their use. Recent analytical work (ref. 9) has proposed that the velocity distribution in the inner region reduces to one universal curve when plotted in the U/U_τ - yU_τ/ν coordinate system. The present analysis, however, does not support the hypothesis that U/U_τ is a

function of yU_τ/ν only, although the present analysis is in good agreement with experimental data in this inner region.

The data of figure 1 are replotted for the inner region in terms of U/U_τ and yU_τ/ν in figure 5. The predicted distributions of figure 1 are also converted to the new coordinates and are shown as the solid curves on figure 5. Also included in figure 5 (dashed curves) is the faired distribution given by reference 9 as the best representation of a great number of experimental profiles. The linear relation $U/U_\tau = yU_\tau/\nu$ is included as a reference curve on figure 5. In all cases the prediction of equation (5) appears equal to or better than the curve of reference 9. Obviously, the experimental data presented in figure 5 do not suggest one universal curve for all turbulent profiles.

Although the present relation does not give the linear relation $U/U_\tau = yU_\tau/\nu$, it may be shown to approach this linear relation. Equation (5) may be rewritten, using the binomial series, in order to allow a closer look at the "low" powers of (y/δ). In terms of U/U_τ the equation may be written as

$$\frac{U}{U_\tau} = \frac{yU_\tau}{\nu} + \frac{yU_\tau}{2\nu}\left\{(1 - 2n - m)\left(\frac{y}{\delta}\right) + \left[\frac{2}{3} + \frac{8n^3 - 10n^2 - 3m^2 - m^3}{3(2n - m)}\right]\left(\frac{y}{\delta}\right)^2 + \cdots\right\} + \frac{U_1}{U_\tau} nm \left\{\left(\frac{y}{\delta}\right)^2 + \frac{(3 - 2n - m)}{3}\left(\frac{y}{\delta}\right)^3 + \cdots\right\} \tag{18}$$

To first order in y, $U/U_\tau = yU_\tau/\nu$; however, second and higher order velocity derivatives are predicted at $y = 0$.

The existence of the second velocity derivative at the wall is objectionable since it is considered essential that it vanish for the flat-plate case (see ref. 14). The second derivative at the wall was shown in reference 3 to give a reasonable interpolation for the measured turbulent shear stress to the wall. However, the approach of the turbulent shear stress to the wall as the fourth power of the distance (logically deduced in ref. 15) stands as an objection to the present relation. The first derivative, unlike the second, fits the boundary condition, and also fits the data over most of the layer, although there are some limited regions where the deviation from data is detectable. The velocity distribution itself fits the data well, and therefore all integrals derived from the velocity distribution are expected to give adequate accuracy.

Separation Region

In order to attach physical significance to the present results at separation, the model pictured for the boundary layer must be expanded. Separation is believed to begin in a very intermittent way, such as observed in waterflow (ref. 12). This intermittent separation region may have a time average shear stress at the wall; although as will be seen, the velocity distribution is more or less independent of the wall conditions. It is assumed that the inner region, which depends greatly on wall conditions, vanishes at the start of intermittent separation. The vanishing of the inner or sublayer agrees with the concept that it decreases in thickness as the x-Reynolds number increases. The appearance of the constant virtual viscosity boundary layer can be postulated to be the beginning of intermittent separation.

The sequence of flow events beyond the beginning of intermittent separation is not treated. It can be concluded that two-dimensional separation with skin friction equal to zero occurs somewhere downstream of the start of intermittent separation. Further downstream a region of reverse flow might also be expected.

Because of the above suggestions, the case of wall shear stress equal to zero is not considered as a criterion for separation, but rather, the special case of equation (5), in which the $2n$ power term is neglected, will be considered. Mathematically this is done by taking the limit of equation (5) as $2n$ approaches infinity. The simple profile

$$\frac{U}{U_1} = 1 - \left(1 - \frac{y}{\delta}\right)^n \tag{19}$$

results. (Eq. (19) was first implied from the evaluation of the separation profile (fig. 1(d)).) With the use of equations (13) and (17) to evaluate m and ζ, a value of -1.00 for ζ was obtained. Note that equation (19) with $m = 2$ is the exact solution for laminar flow in a channel, Poiseuille flow. With $m = 1$ equation (19) is the Couette flow solution. A value of s may be obtained from the derivative of equation (19), $s = m/2$. The hypothesis that $s = 0$ at separation is not required by equation (19). The value of wall shear stress does not enter into the calculation of the velocity distribution as specified by equation (19) because of the reduction of the inner layer to a negligibly small region.

If equation (19) can be accepted as representative of flow at separation, it leads to a unique relation between momentum, displacement, and boundary-layer thickness

$$\frac{\delta^*}{\theta} = 1 + \frac{1}{1 - \frac{\delta^*}{\delta}} \tag{20}$$

Equation (20) may be used as the criterion for the onset of intermittent separation. At a given value of δ^*/δ, profiles with values of the form factor δ^*/θ greater than that predicted by equation (20) will be separated. A plot of equation (20) is shown as the dashed curve on figure 6. Experimental values of the form factor δ^*/θ and δ^*/δ for profiles measured near the start of turbulent separation are plotted on figure 6. These measured points are for several different flow configurations. In all cases the predicted criterion seems quite reasonable and is within the limits of uncertainty of measurement as to where separation is occurring.

The insert on figure 6 shows data (ref. 20) for the flow in an axisymmetric diffuser. (Only the data in and approaching the separation region are plotted.) No statement about separation was made for the data of reference 20; however, if the values of skin-friction coefficient listed in table II of reference 20 are plotted against x, it is noted that a definite break occurs in the curves near $C_f = 0.0004$. It was arbitrarily assumed that $C_f = 0.0004$ represents the onset of intermittent separation. The insert in figure 6 shows that the assumption for the onset of separation corresponds to the predictions of equation (20).

An approximate method of treating shock-induced turbulent separation based on knowledge of the form factor before and after the separation is made in reference 21. A one-seventh power profile was selected ($\delta^*/\delta = 0.1250$) as being representative of flat-plate turbulent boundary layers. This gives a form factor of 1.286 before separation. In order to correlate shock-induced turbulent separation measurements reference 21 selected a value of $H = 2.2$. The present criterion for separation, using the same value of δ^*/δ, would predict $H = 2.143$ at separation, and the point at $\delta^*/\delta = 0.1250$ (ref. 21) is included on figure 6; the agreement is seen to be good.

THE LAMINAR BOUNDARY LAYER

Equation for the Laminar Boundary Layer

For laminar flow it is possible to simplify the general equation. No longer do two separate power terms seem necessary to account for two different boundary-layer regions. Several possible mathematical conditions may be imposed on equation (5) in order to eliminate one of the unknowns. One method, self evident from attempts to fit laminar profiles, is that $2n = m$; this is an indeterminate point of equation (5). Taking the limit of equation (5) as $2n \to m$ yields the following relation (s and δ being held constant):

$$\frac{U}{U_1} = 1 - \left(1 - \frac{y}{\delta}\right)^m \left[(2s - m)\log 1 - \frac{y}{\delta} + 1\right] \qquad (21)$$

Another possibility $2s = m$ (or $2n$) would also eliminate one of the power terms from equation (5). However, the same result is obtained if $2s = m$ is required in equation (21).

$$\frac{U}{U_1} = 1 - \left(1 - \frac{y}{\delta}\right)^m \tag{22}$$

Thus, equation (21) is a more general relation than equation (22). Equation (22) is identical to equation (19). Equation (22) is an easily identified equation for laminar flow in that it contains several exact solutions.

$m = 0$ (Potential flow)

$m = 1$ (Laminar Couette flow)

$m = 2$ (Laminar Poiseuille flow)

Equation (22) may also serve as a first approximation to laminar boundary-layer flow, however, the restriction $2s = m$ is not exact for boundary-layer flow. Equation (21) has been considered the most logical choice to represent laminar boundary layers.

The skin-friction parameters may be expressed in terms of the free-stream pressure gradient by employing the boundary condition at $y = 0$.

$$\mu \frac{\partial^2 U}{\partial y^2} = \frac{\partial p}{\partial x} = -\rho U_1 \frac{dU_1}{dx} \tag{23}$$

(This boundary condition was useable only for the laminar case of eq. (5).) The following relation between s, m, and δ is obtained by using condition (23):

$$2s = \frac{\frac{\delta^2}{\nu}\frac{dU_1}{dx} + m^2}{(2m - 1)} = \frac{\lambda + m^2}{(2m - 1)} \tag{24}$$

where $(\delta^2/\nu)(dU_1/dx)$ is the well-known Pohlhausen pressure-gradient parameter λ. Equation (21) is reduced to a two-parameter (m and δ) family of curves by using equation (24)

$$\frac{U}{U_1} = 1 + \left(1 - \frac{y}{\delta}\right)^m \left[\frac{m(m - 1) - \lambda}{(2m - 1)} \log\left(1 - \frac{y}{\delta}\right) - 1\right] \tag{25}$$

The need for two parameters to represent adequately laminar velocity distributions was pointed out in reference 22. A one-parameter family, such as the Pohlhausen fourth-degree polynomial, gives reasonably accurate

solutions in a region of accelerated flow, but its adequacy in a region of retarded flow may be quite poor. Equation (22) is also objectionable from this standpoint.

The relations for displacement and momentum thickness are

$$\frac{\delta^*}{\delta} = \frac{m(m-1)-\lambda}{(2m-1)(m+1)^2} + \frac{1}{(m+1)} \tag{26}$$

$$\frac{\theta}{\delta} = \frac{m(m-1)-\lambda}{(2m-1)(m+1)^2} + \frac{m}{(2m+1)(m+1)} - \frac{2[m(m-1)-\lambda]}{(2m-1)(2m+1)^2} - \frac{2[m(m-1)-\lambda]^2}{(2m-1)^2(2m+1)^3} \tag{27}$$

Equation (25) could be used with the momentum-integral and energy-integral equations (see, for instance, ref. 22) to obtain an approximate solution for the complete laminar boundary layer. However, since the present report aims to demonstrate the ability of the equation to represent the velocity profile, the tedious process of solving the complete equations was not undertaken.

Comparison with the Blasius Flat-Plate Velocity Distribution

The present relation can be compared with the Blasius profile by assuming a value for the boundary-layer thickness δ:

$$\delta = 5.2\sqrt{\frac{\nu x}{U_1}} \tag{28}$$

This thickness corresponds to a velocity ratio of $U/U_1 = 0.994$ for the Blasius profile. The parameter m is now computed from the momentum equation, which for a flat plate is

$$\frac{d\theta}{dx} = \frac{\tau_w}{\rho U_1^2} = \frac{2s\nu}{\delta U_1} = \frac{m^2\nu}{\delta U_1(2m-1)} \tag{29}$$

and

$$\frac{d\theta}{dx} = \frac{d\delta}{dx}\alpha \quad (\lambda = 0, \text{ flat plate}) \tag{30}$$

where $\alpha = \theta/\delta$, as expressed by equation (27) with $\lambda = 0$. When $\delta = 0$ at $x = 0$, the momentum equation is integrated to give

$$\delta = \sqrt{\frac{2m^2}{\alpha(2m - 1)}}\sqrt{\frac{x}{U_1}} \tag{31}$$

Equation (31) together with equation (28) can be solved to give a value of $m = 2.86$.

With the substitution of the value for m into equation (25) and the setting of $\lambda = 0$, the flat-plate laminar boundary-layer velocity profile becomes

$$\frac{U}{U_1} = 1 + \left(1 - \frac{y}{\delta}\right)^{2.86}\left[1.13 \log\left(1 - \frac{y}{\delta}\right) - 1\right] \tag{32}$$

The profile of equation (32) is compared with the Blasius profile in figure 7; for the Blasius case the relation $y/\delta = \eta/5.2$ was used. A comparison of the parameters computed for the present profile with the exact values of Blasius is as follows:

	Present analysis	Exact values (Blasius)
C_f	$1.33 \frac{\nu}{U_1 L}$	$1.328 \frac{\nu}{U L}$
θ	$0.664 \frac{\nu x}{U_1}$	$0.664 \frac{\nu x}{U}$
δ^*	$1.74 \frac{\nu x}{U_1}$	$1.729 \frac{\nu x}{U}$

The comparison of equation (32) with the Blasius profile is certainly satisfactory, and the assumption used in arriving at the laminar equation appears reasonable at least for the flat-plate case.

In the section Similarity of the Outer Region of the Turbulent Boundary Layer, it was demonstrated that the velocity distribution in terms of $\frac{U_1 - U}{U_\tau}$ is approximated by a simple power relation, equation (15). A simple method can be suggested for determination of the power m of turbulent profiles from equivalent laminar flows. Consideration of equation (22) with the momentum equation (29) requires that $2s = m$ and

$\alpha = \frac{m}{(m + 1)(m + 2)}$. The equation for δ, equivalent to equation (31), is

$$\delta = \left[\sqrt{2(m + 1)(2m + 1)}\right]\sqrt{\frac{\nu x}{U_1}} \tag{33}$$

For the Blasius case $\delta = 5.2\sqrt{\nu x/U_1}$, it is found that $m = 1.86$. This value of m may be compared with the values of $m = 1.8$ and 1.9 shown in figure 3 for the outer region of the turbulent boundary layer.

A comparison of the laminar equation (32) with the turbulent equation (15) ($m = 1.9$) is shown as an insert in figure 7. The similarity coordinate for turbulent boundary layers $\frac{U - U_1}{U_\tau}$ is used for the plot. The laminar profile, equation (32), was transformed to this coordinate system by using the constant $(\sqrt{k})\sqrt{\eta^* \frac{U'(0)}{U_1}}$ (ref. 2, see ordinate of insert of fig. 10). The change due to the apparent difference in viscosity is accounted for by the k, which was equal to 0.018 (ref. 2). The value of η at $y = \delta^*$ in the laminar boundary layer is η^*, and $U'(0)$ is the derivative of U with respect to η at $\eta = 0$. For the present transformation this constant $(\sqrt{k})\sqrt{\eta^* \frac{U'(0)}{U_1}}$ was 0.102. Good agreement is obtained between the profile from the equation for mean velocity in a turbulent layer (eq. (15)) and that for an equivalent laminar layer obtained by proper transformation of equation (32).

Comparison with the Laminar Separation Profiles

As in the turbulent boundary-layer case, a consideration of the separation region of the laminar boundary layer is of prime importance. Laminar flow separation seems well defined as the point where $s = 0$. The condition $s = 0$ leads to a simplification of the velocity equation (21), and also yields a relation for form factor δ^*/θ as a function of the Pohlhausen pressure gradient parameter.

For $s = 0$, equation (24) gives the following relation of m and λ:

$$m = \pm\sqrt{-\lambda} \tag{34}$$

and equation (24) reduces to (only the plus sign gave physically real results):

$$\frac{U}{U_1} = 1 + \left(1 - \frac{y}{\delta}\right)^{\sqrt{-\lambda}}\left[\sqrt{-\lambda}\,\log\left(1 - \frac{y}{\delta}\right) - 1\right] \tag{35}$$

This separation equation does not require a particular value of λ at separation, but agrees with the fact that separation occurs over a range of λ between approximately -5 to -12.

The relations for displacement and momentum thickness become

$$\frac{\delta^*}{\delta} = \frac{2\sqrt{-\lambda} + 1}{(\sqrt{-\lambda} + 1)^2} \tag{36}$$

$$\frac{\theta}{\delta} = \frac{(2\sqrt{-\lambda} + 1)}{(\sqrt{-\lambda} + 1)^2} - \frac{2(\sqrt{-\lambda})^2}{(2\sqrt{-\lambda} + 1)^3} - \frac{2\sqrt{-\lambda}}{(2\sqrt{-\lambda} + 1)^2} - \frac{1}{(2\sqrt{-\lambda} + 1)} \tag{37}$$

Equation (35) is compared with several different laminar separation profiles in figure 8. The value of λ in each case was taken either from stated values or from information known about the profile being compared. (For the theoretical profiles δ is taken at $U/U_1 = 0.995$ to compute λ.) Figure 8(a) compares the present prediction and that of the Pohlhausen equation for $\lambda = -12$. In figures 8(b) and (c) the theoretical profiles computed in references 23 and 24 for different particular pressure gradients are compared with the present relation. Figure 8(d) compares the present relation with actual measurements made in the separation region of an elliptic cylinder (ref. 25).

The agreement of the present profile with the two theoretical profiles is quite poor. There is, of course, a possibility that the theoretical profiles are questionable in that they depend on the basic boundary-layer assumption that conditions change very slowly in the x-direction. This assumption is not generally valid in the separation region. Both the Pohlhausen and the present profile are independent of this condition. The prediction of the experimentally measured separation profile (fig. 8(d)) is much better than in the case of the theoretical profiles, although the predictions are slightly lower than the measured points. The present relation would agree almost exactly with the data of reference 25 if λ had been -6 instead of -5.

The form factor δ^*/θ may be expressed as a function of λ by combining equations (36) and (37). This relation is plotted as a function of $\sqrt{-\lambda}$ on figure 9. Values from the separation profiles considered in figure 8 are also shown on figure 9. For the particular profiles considered the prediction of separation is acceptable. The relation indicates that the limiting value of a form factor is 2.67 for $\sqrt{-\lambda} \to \infty$. This limiting value of form factor might be compared with the value of form factor of 2.60 for the Blasius profile.

CONCLUSIONS

A modified form of the velocity relation previously proposed in reference 1 has been studied in order to establish a general relation to represent boundary-layer velocity profiles for both laminar and turbulent flow. The resulting relations are consistent with a reasonable model of the flow and represent experimental velocity profiles quite adequately. Some of the specific conclusions drawn from the present study are:

1. The proposed equation fits measured turbulent boundary-layer velocity profiles quite well.

2. The relation for turbulent boundary layers agrees with the present concepts of similarity in the outer region of the boundary layer in that a one-parameter family of profiles is obtained. A relation of the similarity parameter to the equivalent laminar boundary-layer flow parameters is possible if concepts from reference 2 are followed.

3. The present results are in reasonable agreement with available experimental data over the whole profile, including the region near the wall. It is demonstrated that the logarithmic profile does not represent all experimental data.

4. A unique relation between the profile form factor and the ratio of displacement thickness to boundary-layer thickness is obtained from the present equation for turbulent separation. Comparison with experimental data shows that the relation serves as an accurate criterion for identifying turbulent separation.

5. The general equation reduces to a laminar profile equation which accurately represented the Blasius flow. The laminar profile also checked the Pohlhausen and an experimental separation profile accurately, however, theoretical laminar separation profiles were matched less accurately.

6. A relation obtained for the form factor at laminar separation in terms of the Pohlhausen pressure gradient parameter indicated separation would not occur when the form factor was less than 2.67 (Blasius value 2.60). The criterion proves adequate for the available separation profiles.

Lewis Research Center
National Aeronautics and Space Administration
Cleveland, Ohio, November 19, 1958

APPENDIX A

SYMBOLS

A,B,C	constants
C_f	local wall shear-stress coefficient, $\frac{\tau_w}{\frac{1}{2}\rho U_1^2}$
G	equilibrium boundary-layer profile parameter, eq. (9)
K	constants $\left(\frac{\delta^* - \theta}{\delta^*}\right)\frac{\delta}{\delta^*}$
k	constant to account for turbulent viscosity
L	characteristic length
m	profile parameter depending on outer region of boundary layer
n	profile parameter depending on inner region of boundary layer
p	static pressure
Re	Reynolds number, $\frac{LU_1}{\nu}$
Re_θ	Reynolds number based on momentum thickness, $\frac{U_1\theta}{\nu}$
s	wall shear-stress parameter, $\frac{\delta\tau_w}{2U_1\mu}$
U	local mean velocity
U_1	free-stream mean velocity
U_τ	skin-friction velocity, $\sqrt{\frac{\tau_w}{\rho}}$
X	distance along curved surface of elliptic cylinder
x	direction parallel to boundary and in direction of mean flow
y	direction normal to boundary and approximately normal to mean flow

Δ equilibrium boundary-layer profile parameter, eq. (8)

δ boundary-layer thickness, in.

δ^* boundary-layer displacement thickness, in.

ζ profile weighting function, $\frac{2(s - n)}{2n - m}$

η variable, $y\sqrt{\frac{U_1}{\nu x}}$

θ boundary-layer momentum thickness, in.

λ Pohlhausen pressure-gradient parameter, $\frac{\delta^2}{\nu} \frac{dU_1}{dx}$

μ coefficient of viscosity

ν kinematic viscosity, μ/ρ

ρ density

τ_w local wall shear stress

APPENDIX B

PROFILE CALCULATION PROCEDURE

Equation (5) can be used to compute any turbulent boundary-layer velocity profile once θ/δ, δ^*/δ, and δ are known along with the general flow conditions of the main stream, namely density, viscosity, and velocity. A brief summary of the necessary steps in computing a profile is given in the following procedure:

(1) If no value of skin friction is given, compute s from its definition and the relation for the skin-friction coefficient from reference 7, $C_f = 0.246\times10^{-0.678(\delta^*/\theta)}Re_\theta^{-0.268}$

Thus,

$$s = \frac{\delta U_1}{4\nu} C_f$$

(2) Compute m from equation (13)

$$m = K - 1 + \sqrt{K(K - 1)}$$

where

$$K = \left(\frac{\delta^* - \theta}{\delta^*}\right)\frac{\delta}{\delta^*}$$

(3) Compute ζ from equation (17)

$$\zeta = -(m + 1)\left(\frac{\delta^*}{\delta}\right)$$

(4) Compute n from definition in equation (4)

$$n = \frac{2s + \zeta m}{2(1 + \zeta)}$$

(Use of eq. (17) (the simplified eq. (6)) in the procedure is not mandatory since it is possible to compute n from the exact equation once s is determined. Evaluation of n by either equation will for most profiles give the same answer.)

(5) All parameters of equation (5) are computed in the above steps so the mean velocity can be calculated from equation (5).

REFERENCES

1. Pai, S. I.: On Turbulent Flow Between Parallel Plates. Jour. Appl. Mech., vol. 20, no. 1, Mar. 1953, pp. 109-114.

2. Clauser, Francis H.: The Turbulent Boundary Layer. Vol. IV of Advances in Appl. Mech., Academic Press, Inc., 1956, pp. 1-51.

3. Sandborn, V. A.: An Approximate Equation for the Mean Velocity Distribution in an Incompressible Turbulent Boundary Layer. Proc. Fifth Midwestern Conf. on Fluid Mech., Ann Arbor (Mich.), Apr. 1957, pp. 85-107.

4. Clauser, Francis H.: Turbulent Boundary Layers in Adverse Pressure Gradients. Jour. Aero. Sci., vol. 21, no. 2, Feb. 1954, pp. 91-108.

5. Hunziker, Paul R., and Florio, José S.: On Turbulent Flow and Eddy Heat Transfer Diffusivity in a Pipe. Jour. Aero. Sci., vol. 24, no. 10, Oct. 1957, pp. 782-784.

6. Landweber, L.: Generalization of the Logarithmic Law of the Boundary Layer on a Flat Plate. Reprint No. 151, State Univ. Iowa, Apr. 1957.

7. Ludwieg, H., and Tillmann, W.: Investigation of the Wall-Shearing Stress in Turbulent Boundary Layers. NACA TM 1285, 1950.

8. Sandborn, Virgil A., and Slogar, Raymond J.: Study of the Momentum Distribution of Turbulent Boundary Layers in Adverse Pressure Gradients. NACA TN 3264, 1955.

9. Coles, Donald: The Law of the Wake in the Turbulent Boundary Layer. Jour. Fluid Mech., pt. 2, vol. 1, July 1956, pp. 191-226.

10. Klebanoff, P. S.: Characteristics of Turbulence in a Boundary Layer with Zero Pressure Gradient. NACA Rep. 1247, 1955. (Supersedes NACA TN 3178.)

11. Schubauer, G. B., and Klebanoff, P. S.: Investigation of Separation of the Turbulent Boundary Layer. NACA Rep. 1030, 1951. (Supersedes NACA TN 2133.)

12. Kline, Stephen J.: Some New Conceptions of the Mechanism of Stall in Turbulent Boundary Layers. Jour. Aero. Sci., vol. 24, no. 6, June 1957, pp. 470-471.

13. Klebanoff, P. S., and Diehl, Z. W.: Some Features of Artificially Thickened Fully Developed Turbulent Boundary Layers with Zero Pressure Gradient. NACA Rep. 1110, 1952. (Supersedes NACA TN 2475.)

14. Corrsin, S.: Discussion of Heat Transfer in Turbulent Pipe Flow by P. R. Hunziker. Appl. Mech. Rev., rev. no. 2322, vol. 11, no. 6, June 1958.

15. Elrod, H. G., Jr.: Note on the Turbulent Shear Stress Near a Wall. Jour. Aero. Sci., vol. 24, no. 6, June 1957, pp. 468-469.

16. Sandborn, Virgil A.: Preliminary Experimental Investigation of Low-Speed Turbulent Boundary Layers in Adverse Pressure Gradients. NACA TN 3031, 1953.

17. Newman, B. G.: Some Contributions to the Study of the Turbulent Boundary-Layer Near Separation. Rep. ACA-53, Aero. Res. Consultative Comm. (Australia), Mar. 1951.

18. von Doenhoff, Albert E., and Tetervin, Neal: Determination of General Relations for the Behavior of Turbulent Boundary Layers. NACA Rep. 772, 1943. (Supersedes NACA WR L-382.)

19. Kuethe, A. M., McKee, P. B., and Curry, W. H.: Measurements in the Boundary Layer of a Yawed Wing. NACA TN 1946, 1949.

20. Robertson, J. M., and Holl, J. W.: Effect of Adverse Pressure Gradients on Turbulent Boundary Layers in Axisymmetric Conducts. Paper No. 56-A-25, ASME, June 1956.

21. Reshotko, Eli, and Tucker, Maurice: Effect of a Discontinuity on Turbulent Boundary-Layer-Thickness Parameters with Application to Shock-Induced Separation. NACA TN 3454, 1955.

22. Tani, Itiro: On the Approximate Solution of the Laminar Boundary-Layer Equations. Jour. Aero. Sci., vol. 21, no. 7, July 1954, pp. 487-495.

23. Howarth, L.: On the Solution of the Laminar Boundary Layer Equations. Proc. Roy. Soc. (London), ser. A, vol. 164, no. A919, Feb. 1938, pp. 547-579.

24. Hartree, D. R.: On an Equation Occurring in Falknew and Skan's Approximate Treatment of the Equations of the Boundary Layer. Proc. Cambridge Phil. Soc., pt. 2, vol. 33, Apr. 1937, pp. 223-239.

25. Schubauer, G. B.: Air Flow in a Separating Laminar Boundary Layer. NACA Rep. 527, 1935.

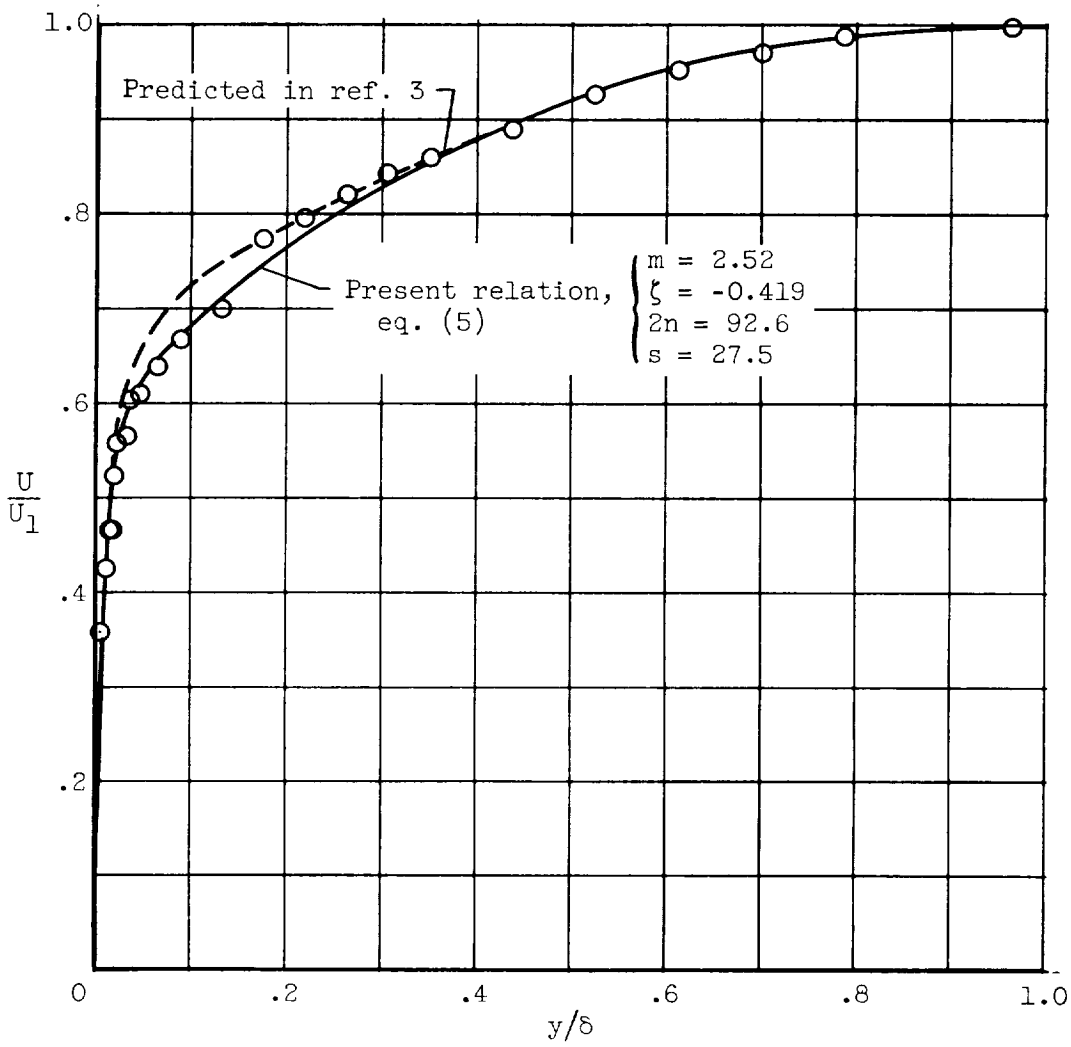

(a) Zero pressure gradient measurement (ref. 8); station 1; free-stream mean velocity, 54.3 feet per second; boundary-layer thickness, 1.15 inches.

Figure 1. - Comparison of equation (5) with turbulent boundary-layer mean velocity measurements.

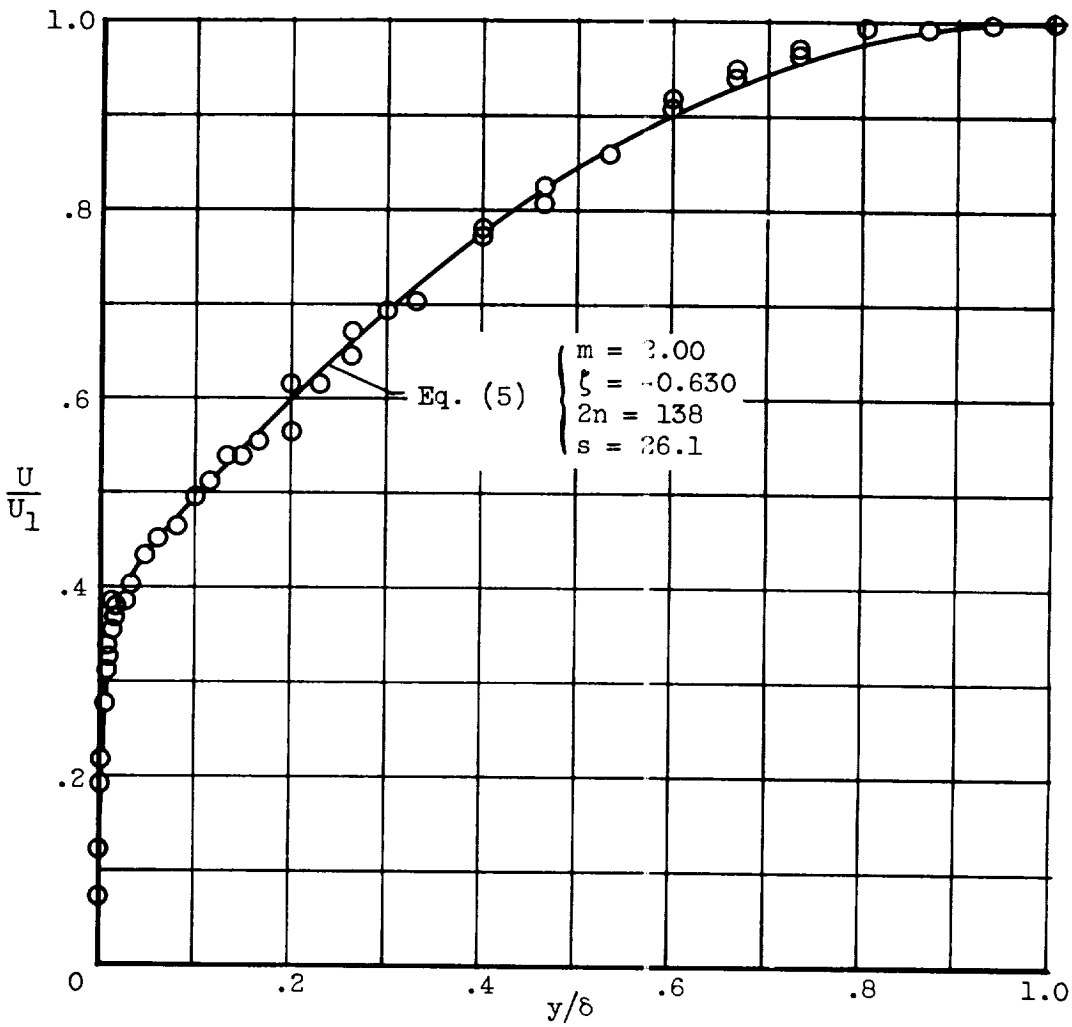

(b) Adverse pressure gradient measurement (ref. 8); station 4; $\partial p/\partial x$ approximately 0.2 pound per square foot per foot; free-stream mean velocity, 42.9 feet per second; boundary-layer thickness, 3.00 inches.

Figure 1. - Continued. Comparison of equation (5) with turbulent boundary-layer mean velocity measurements.

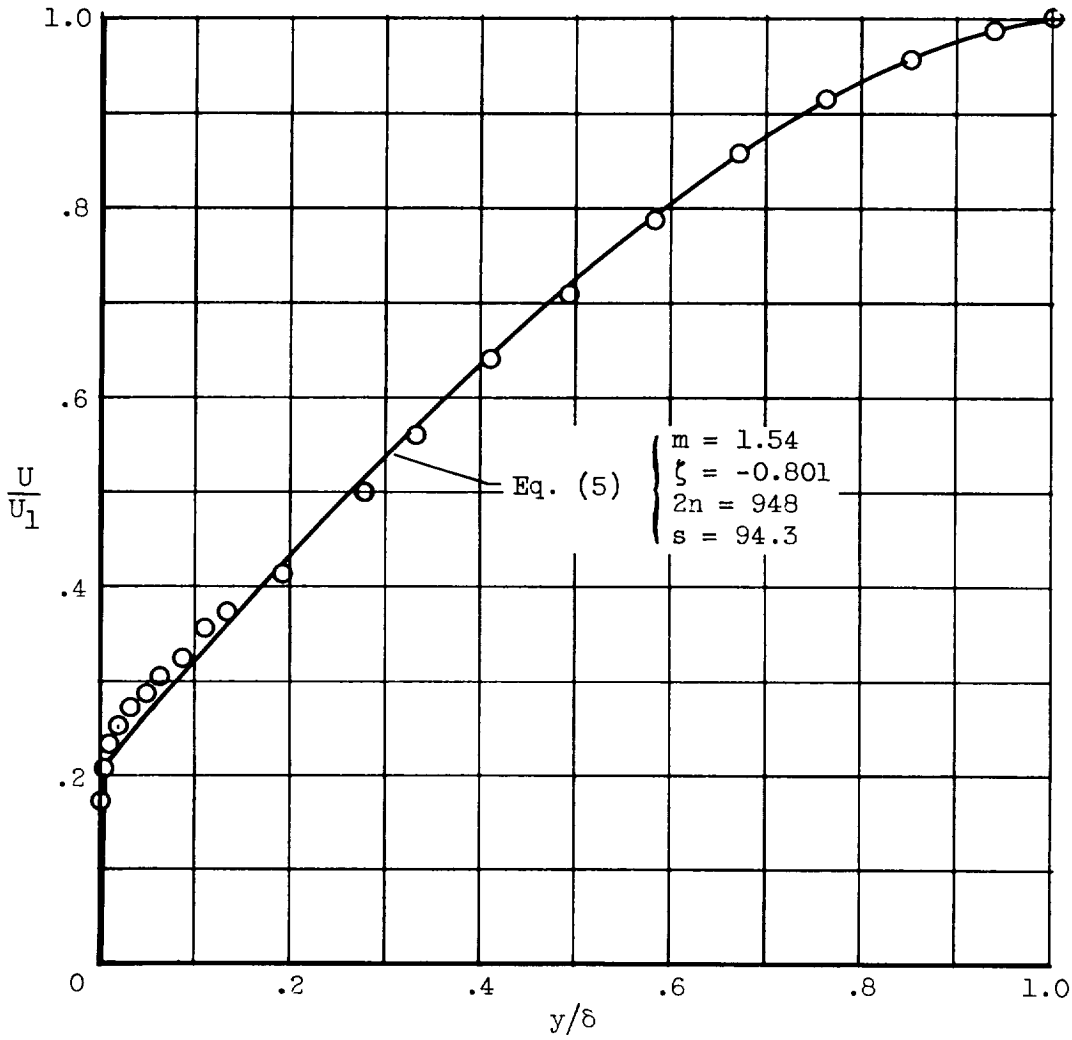

(c) Adverse pressure gradient measurements near separation (x, 24.5 ft; ref. 11).

Figure 1. - Continued. Comparison of equation (5) with turbulent boundary-layer mean velocity measurements.

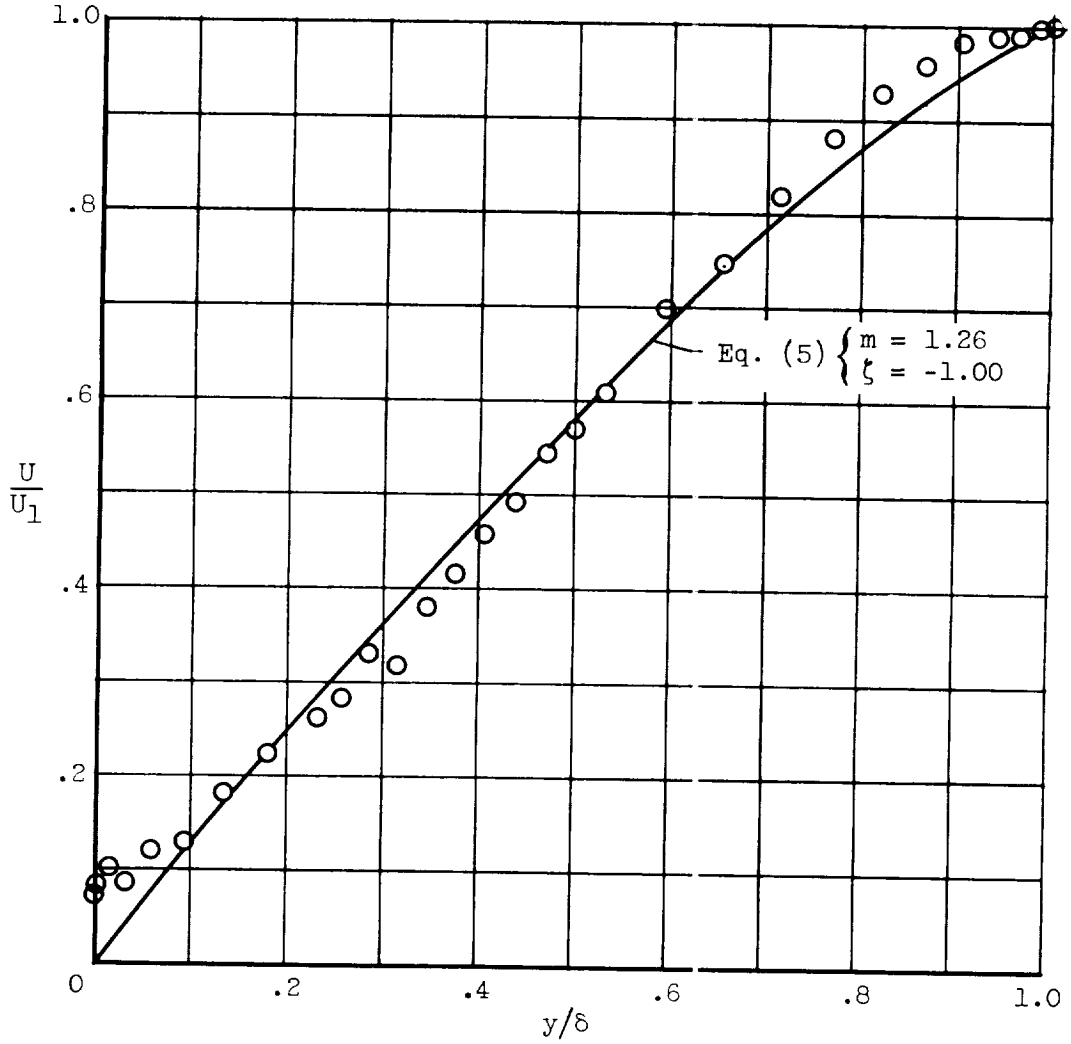

(d) Separation measurement (x, 25.7 ft; ref. 11).

Figure 1. - Continued. Comparison of equation (5) with turbulent boundary-layer mean velocity measurements.

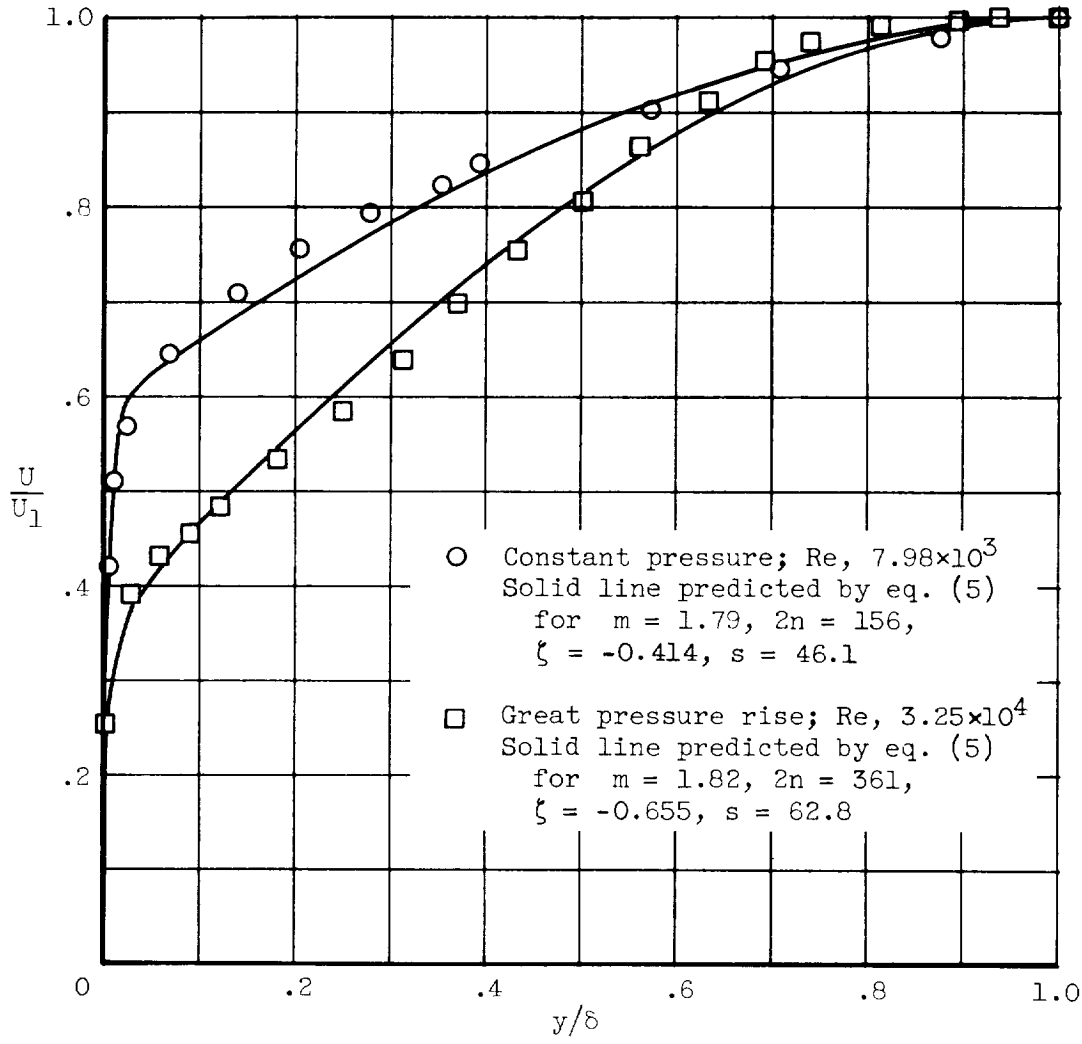

(e) Measurements of reference 7.

Figure 1. - Continued. Comparison of equation (5) with turbulent boundary-layer mean velocity measurements.

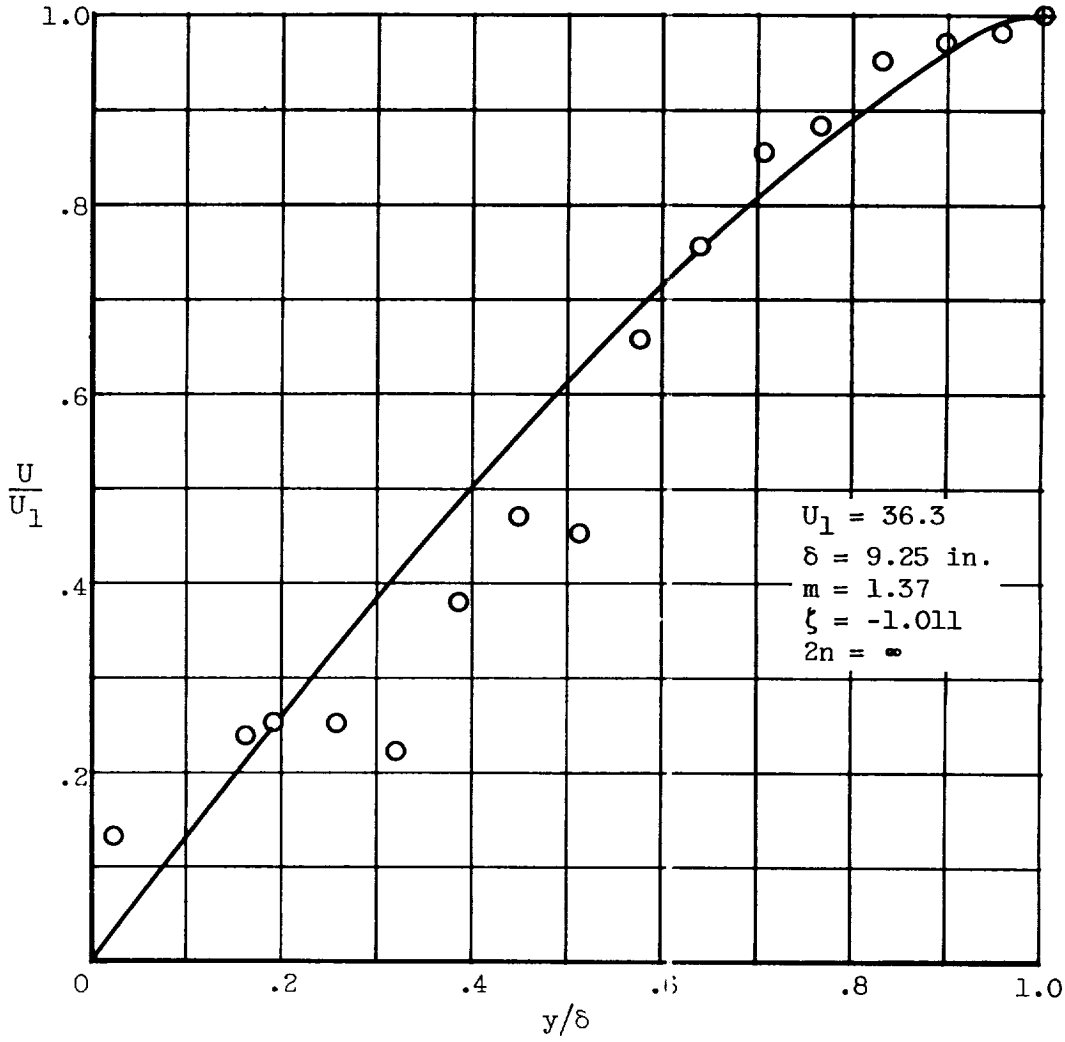

(f) Separation measurement of reference 16.

Figure 1. - Concluded. Comparison of equation (5) with turbulent boundary-layer mean velocity measurements.

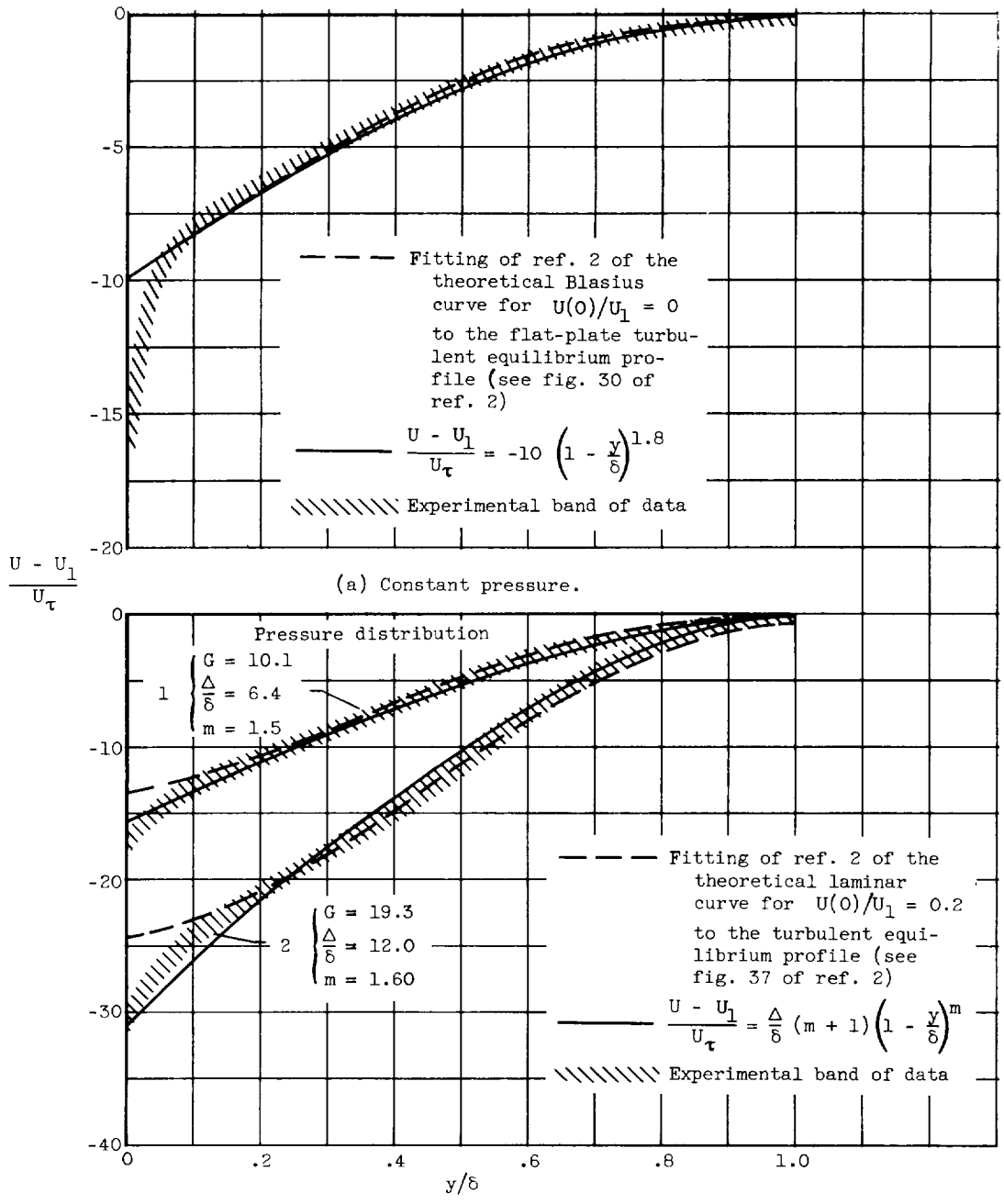

Figure 2. - Comparison of present analysis with outer region similarity.

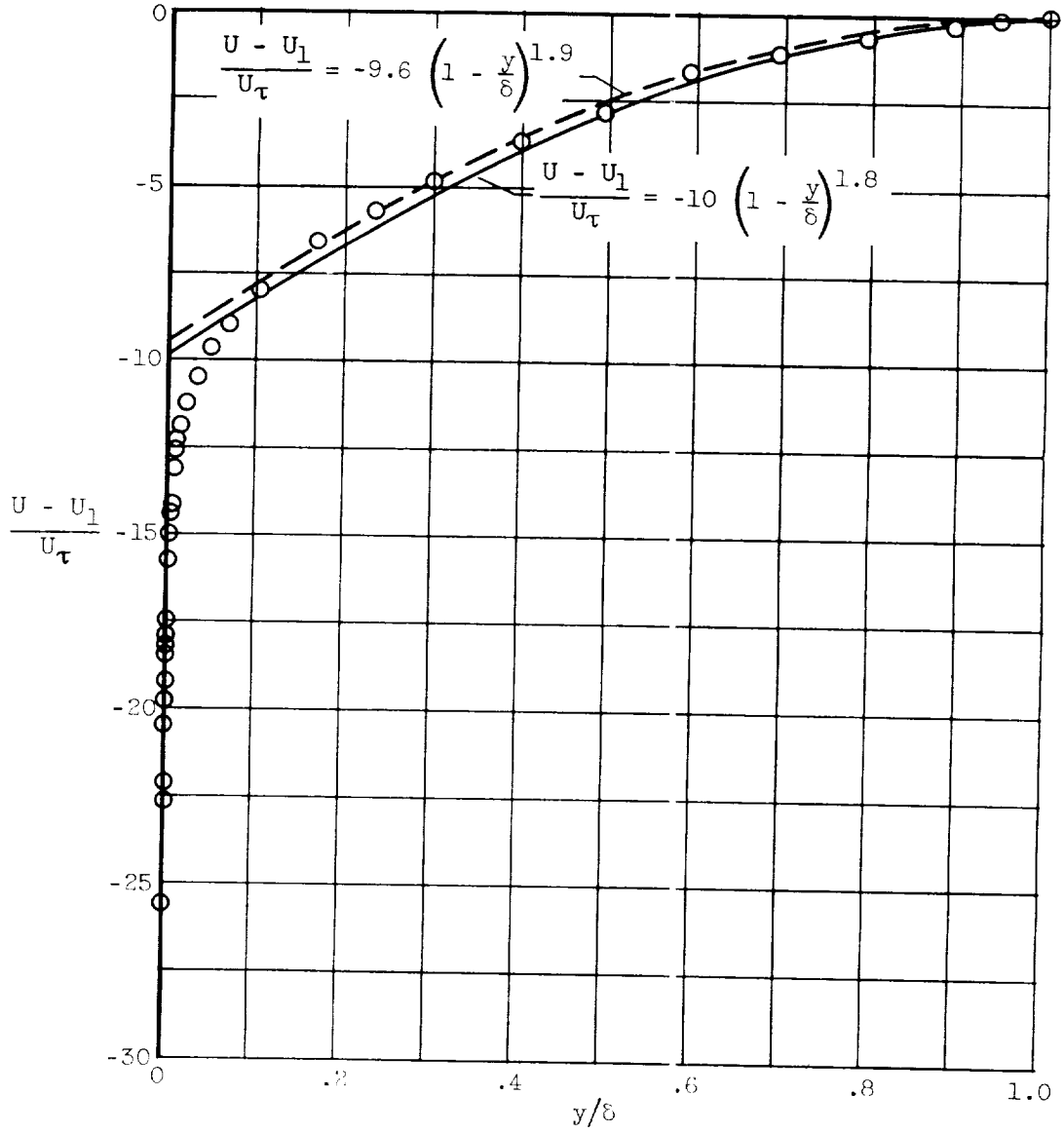

Figure 3. - Comparison of flat-plate similarity profile with measurements of a flat-plate turbulent boundary layer (ref. 10).

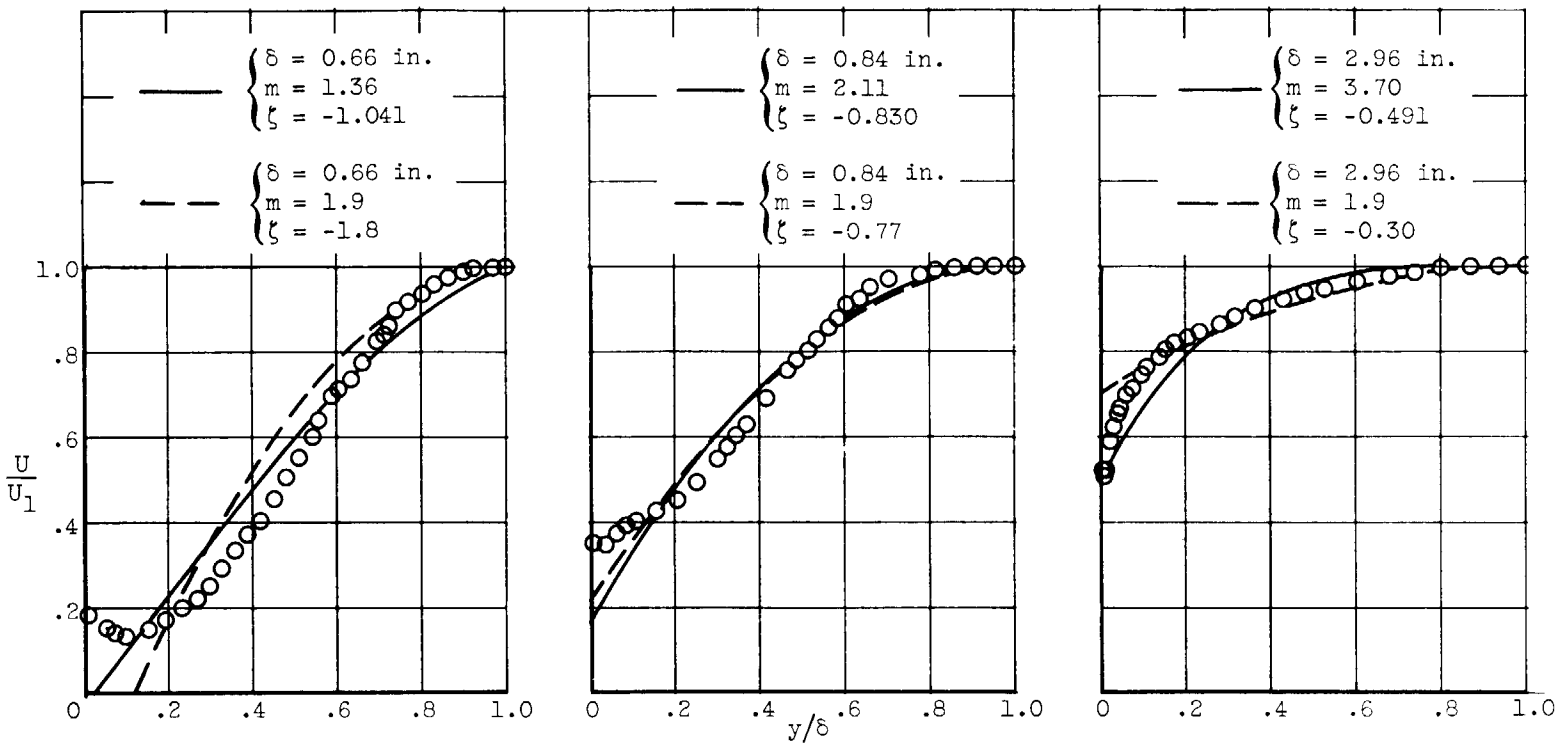

(a) Direction parallel to boundary and in direction of mean flow, 4.17 feet.

(b) Direction parallel to boundary and in direction of mean flow, 4.25 feet.

(c) Direction parallel to boundary and in direction of mean flow, 10.5 feet.

Figure 4. - Comparison of measured boundary-layer profiles downstream of a 0.25-inch cylindrical rod (ref. 13), in contact with surface at x = 4 feet, with predictions of the present equation.

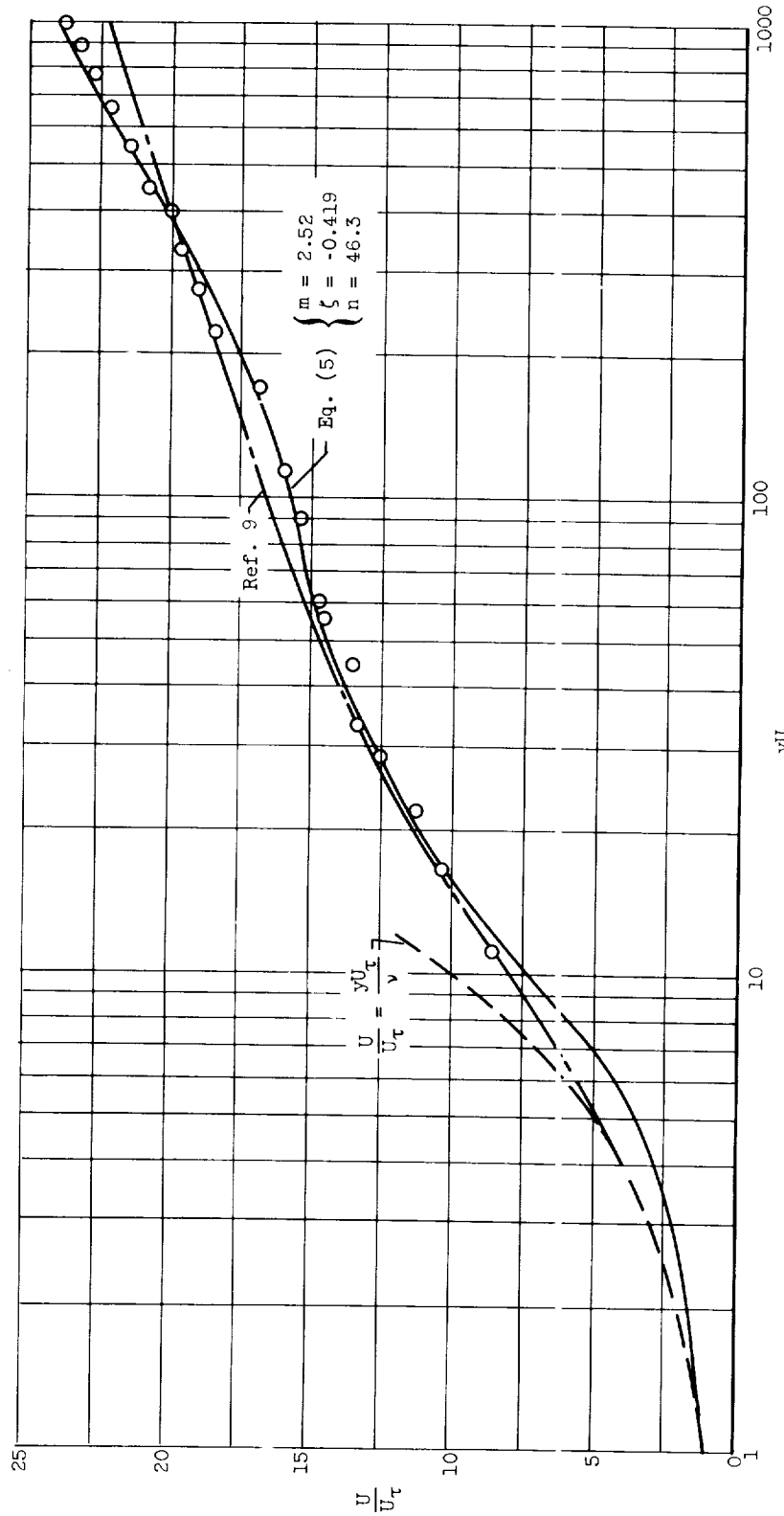

(a) Zero pressure gradient measurement (station 1, ref. 8).

Figure 5. - Comparison of equation (5) with mean velocity measurements in region of the universal logarithmic distribution.

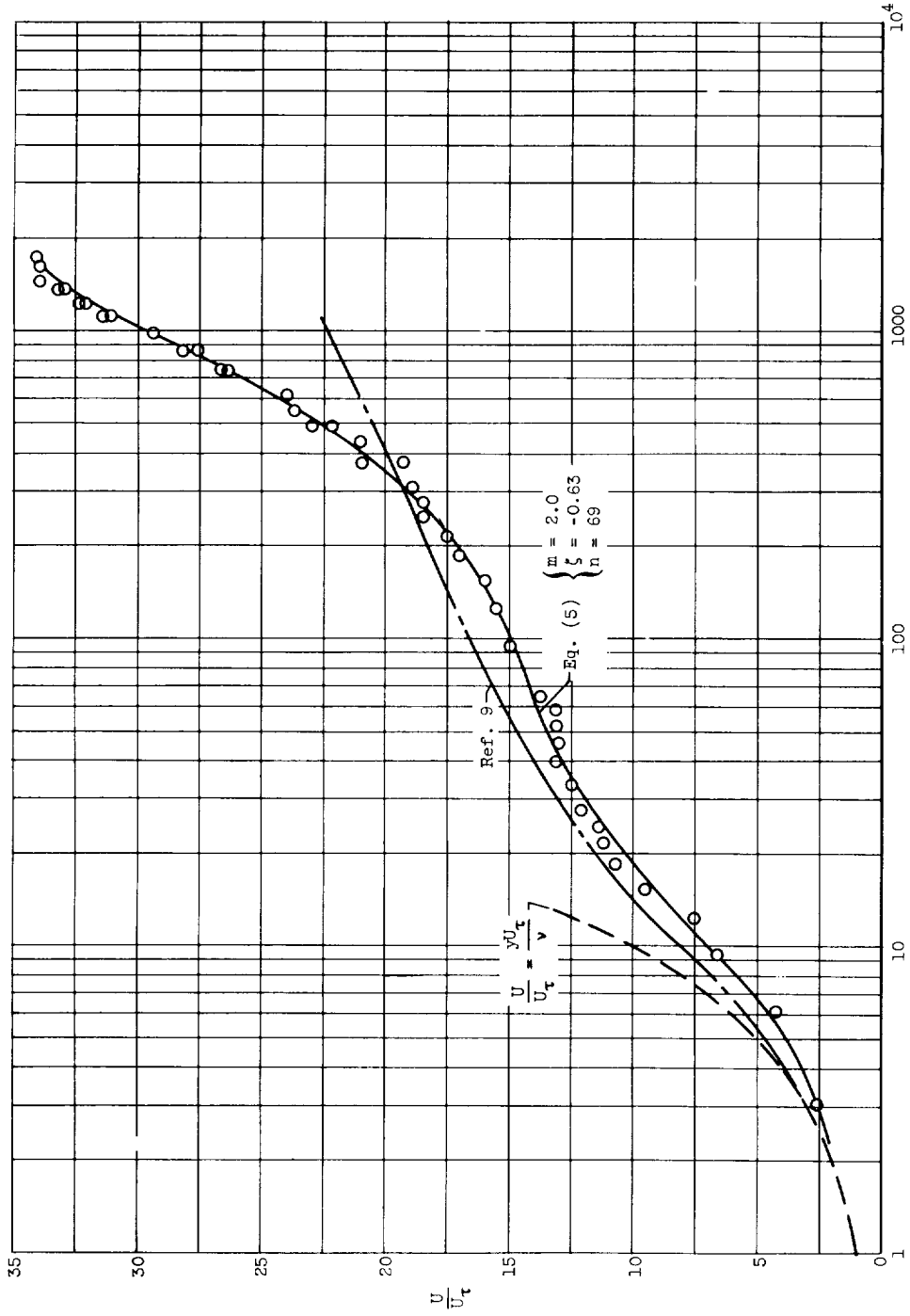

(b) Adverse pressure gradient measurements (station 4, ref. 8).

Figure 5. - Continued. Comparison of equation (5) with mean velocity measurements in region of the universal logarithmic distribution.

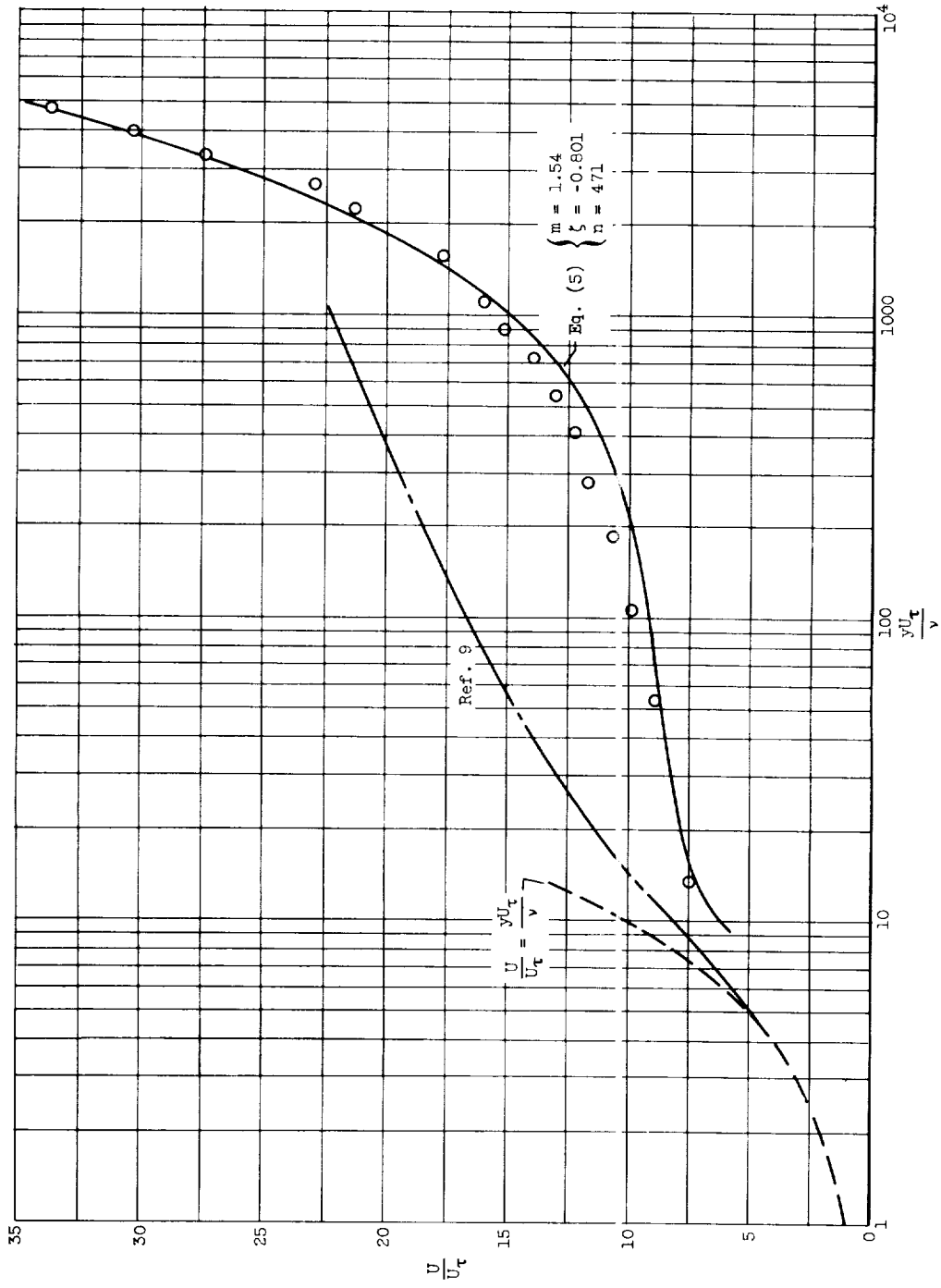

(c) Adverse pressure gradient measurements near separation (x, 24.5 ft, ref. 11).

Figure 5. - Continued. Comparison of equation (5) with mean velocity measurements in region of universal logarithmic distribution.

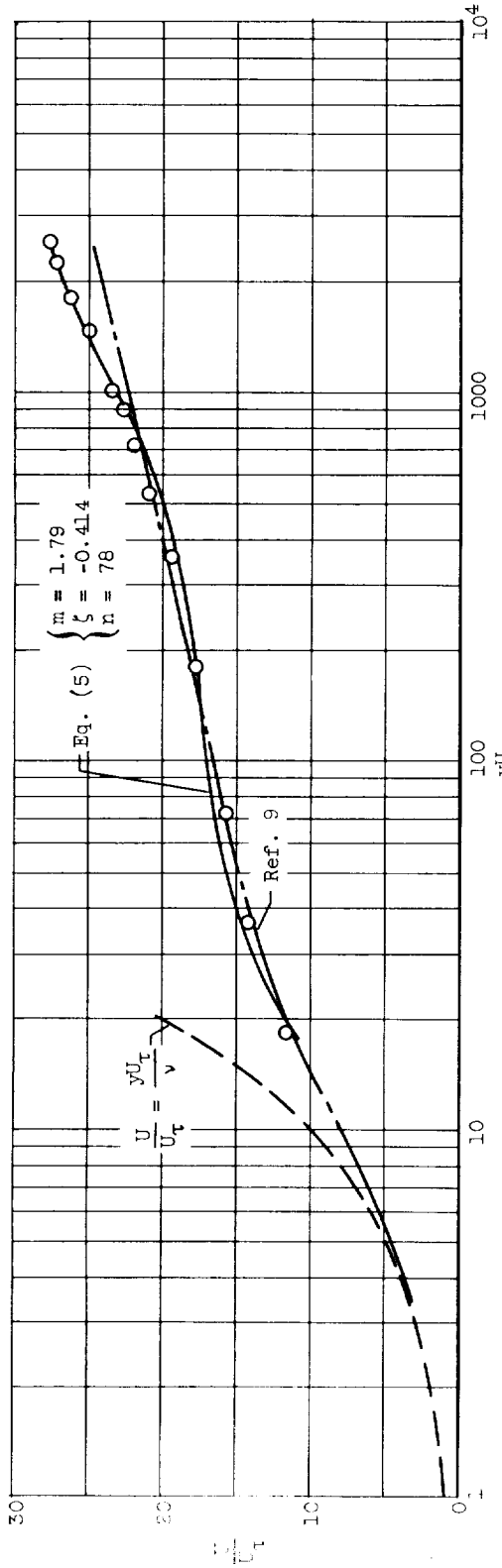

(d) Constant pressure; Re, 7.98×10^3 (ref. 7).

Figure 5. - Continued. Comparison of equation (5) with mean velocity measurements in region of the universal logarithmic distribution.

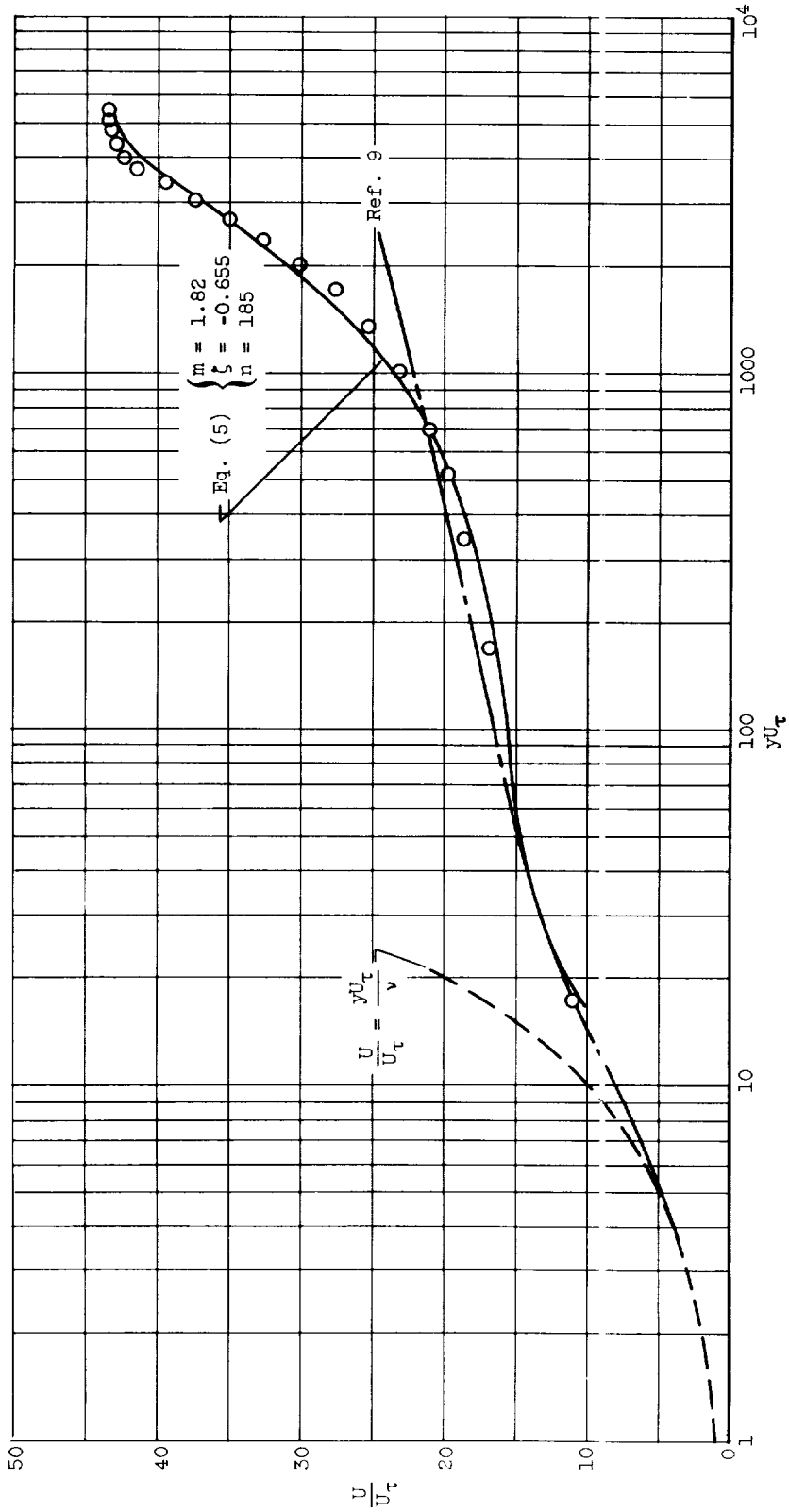

(e) Great pressure rise; Re, 3.25×10^4 (ref. 7).

Figure 5. - Concluded. Comparison of equation (5) with mean velocity measurements in region of the universal logarithmic distribution.

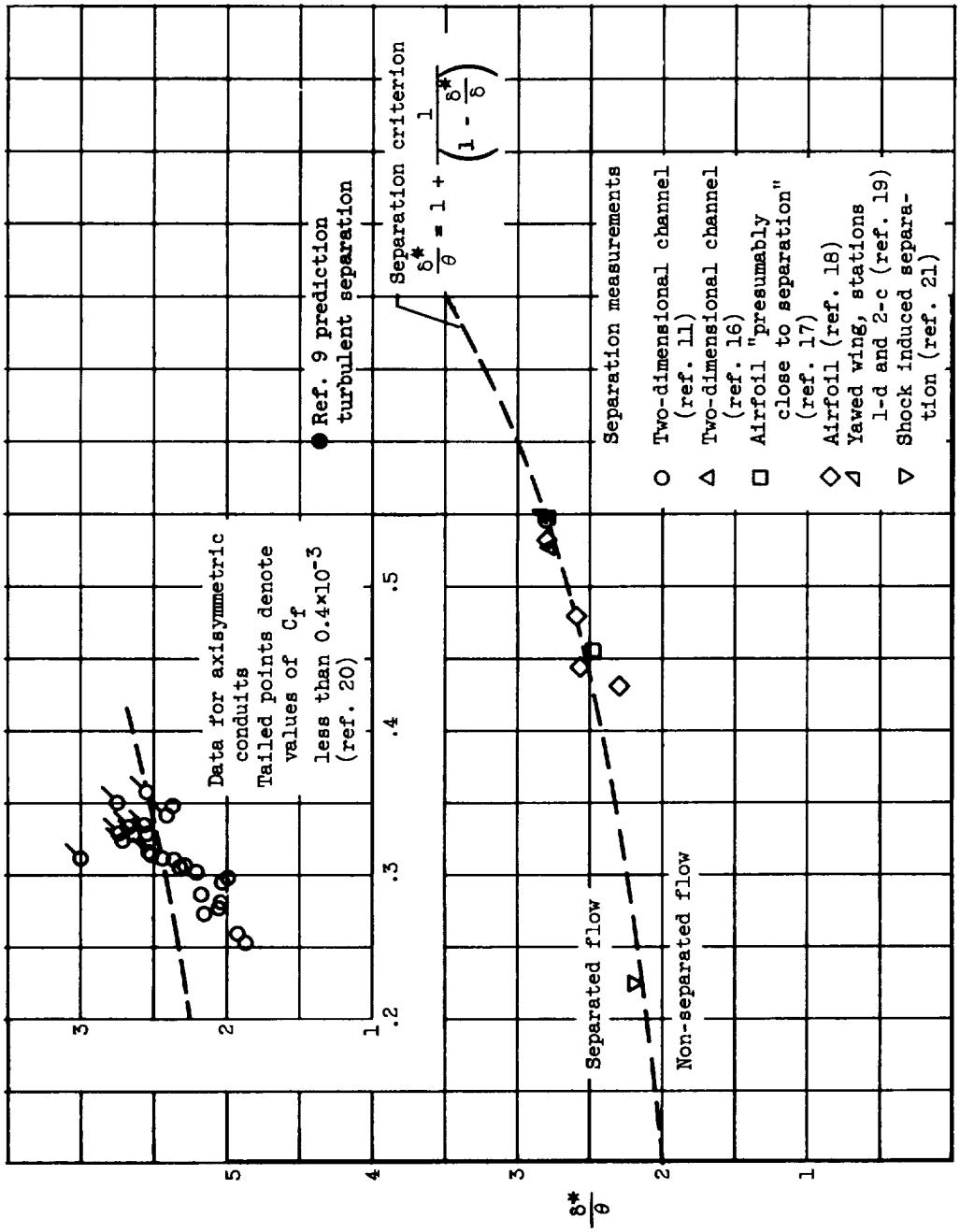

Figure 6. - Comparison of measurements with predicted turbulent separation criterion.

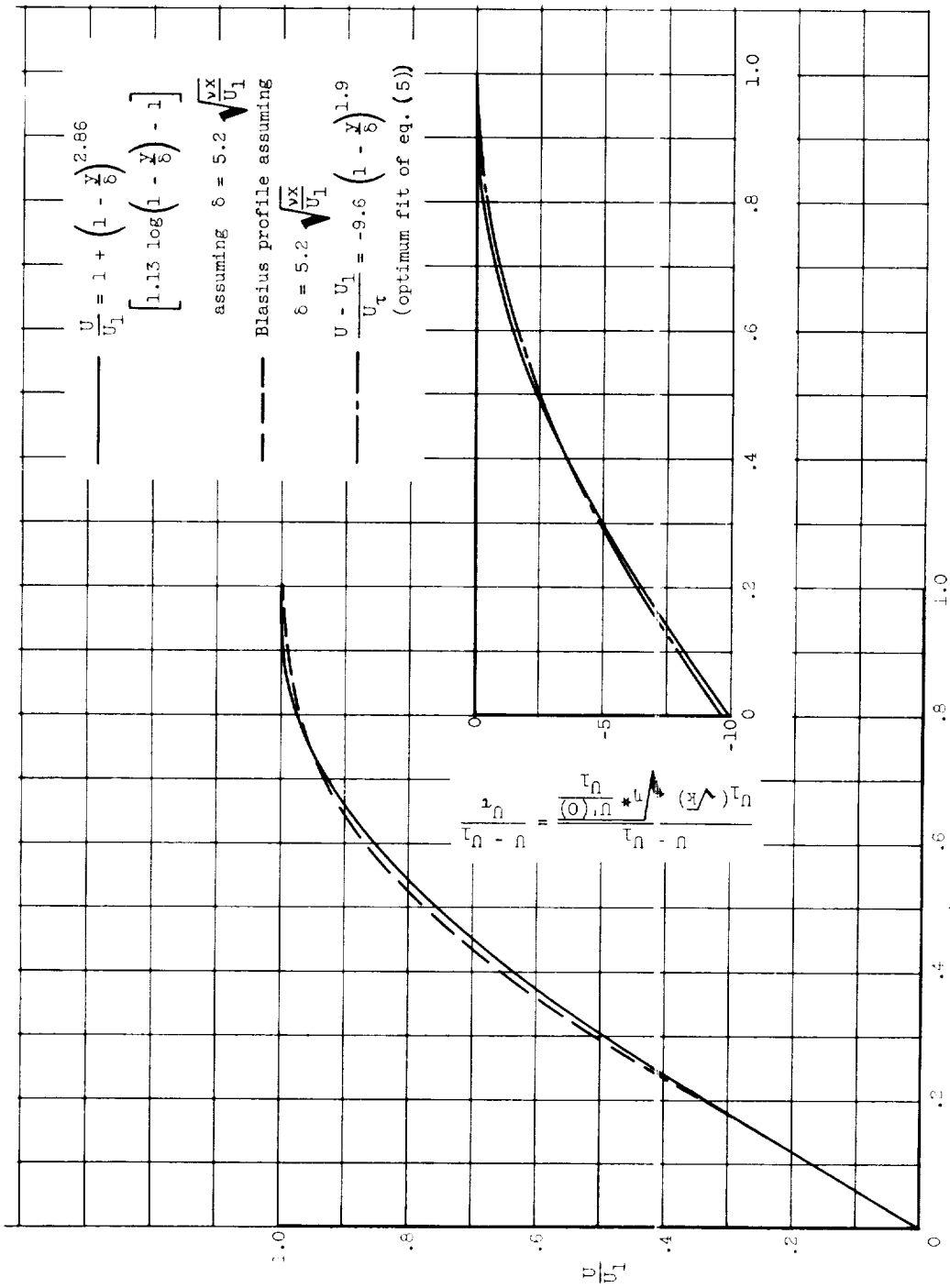

Figure 7. - Comparison of the present equation for the zero pressure gradient laminar velocity profile with the theoretical profile of Blasius and the profile suggested from turbulent similarity considerations.

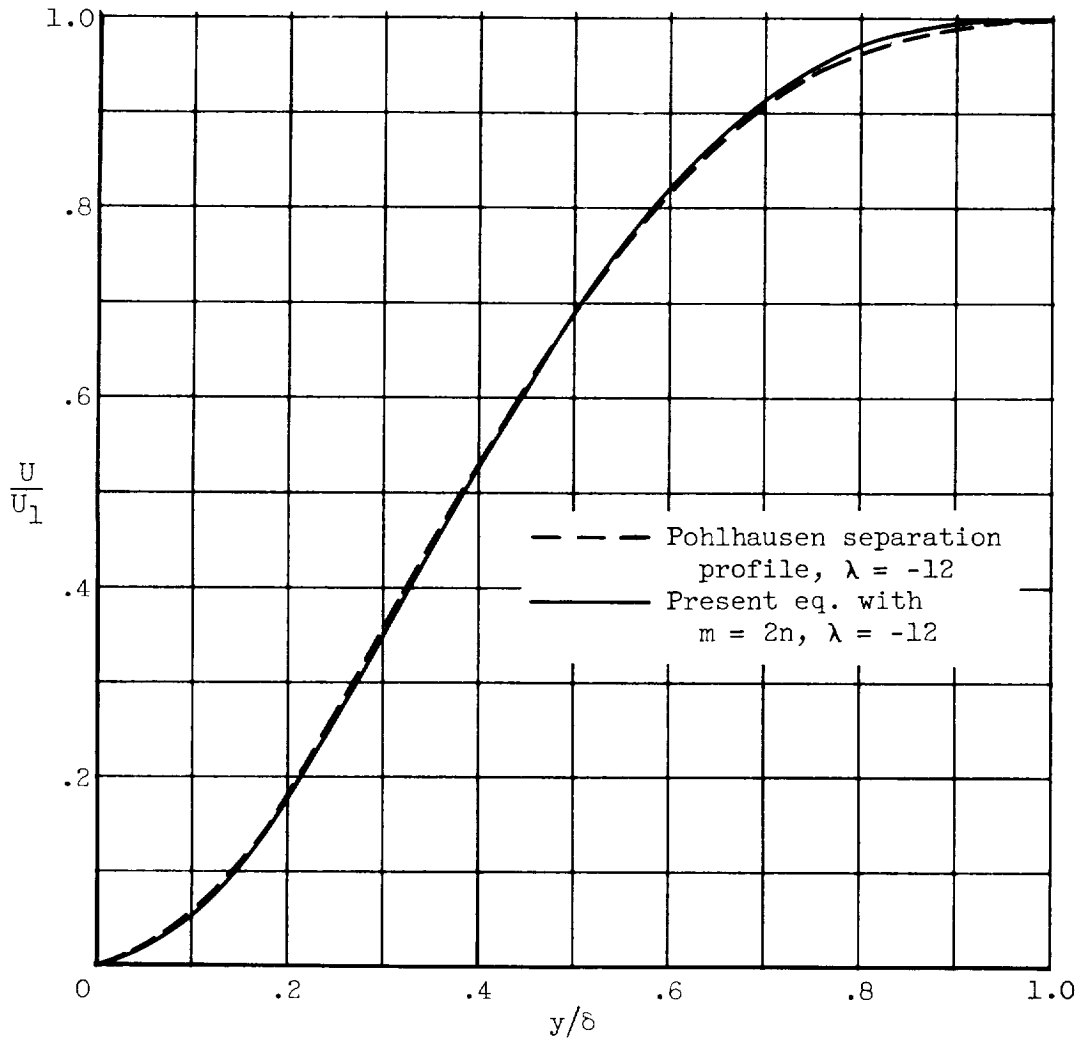

(a) Comparison with the Pohlhausen profile.

Figure 8. - Comparison of the present equation for laminar separation with various profiles.

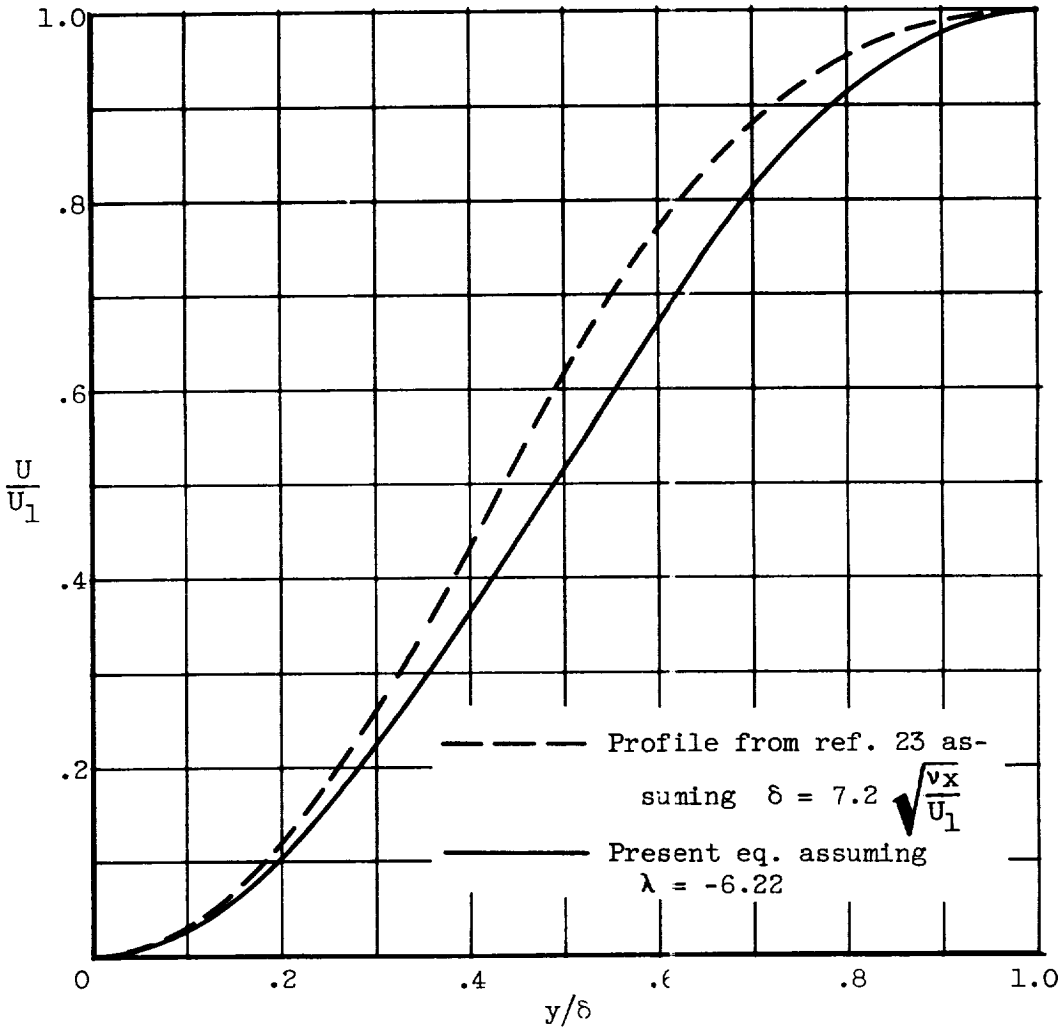

(b) Comparison with the theoretical profile for a linear pressure gradient (ref. 23).

Figure 8. - Continued. Comparison of the present equation for laminar separation with various profiles.

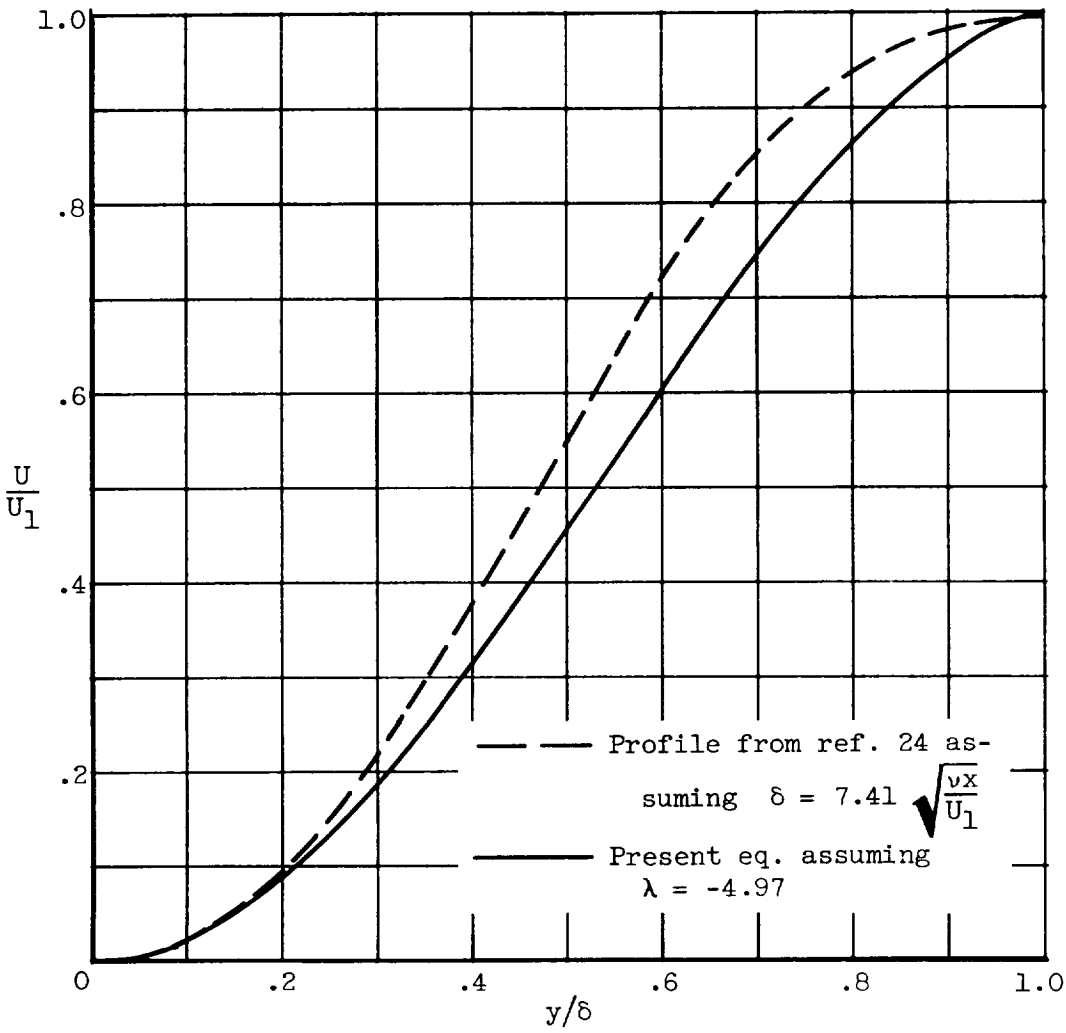

(c) Comparison with the profile for the Falkner-Skan flow separation (ref. 24).

Figure 8. - Continued. Comparison of the present equation for laminar separation with various profiles.

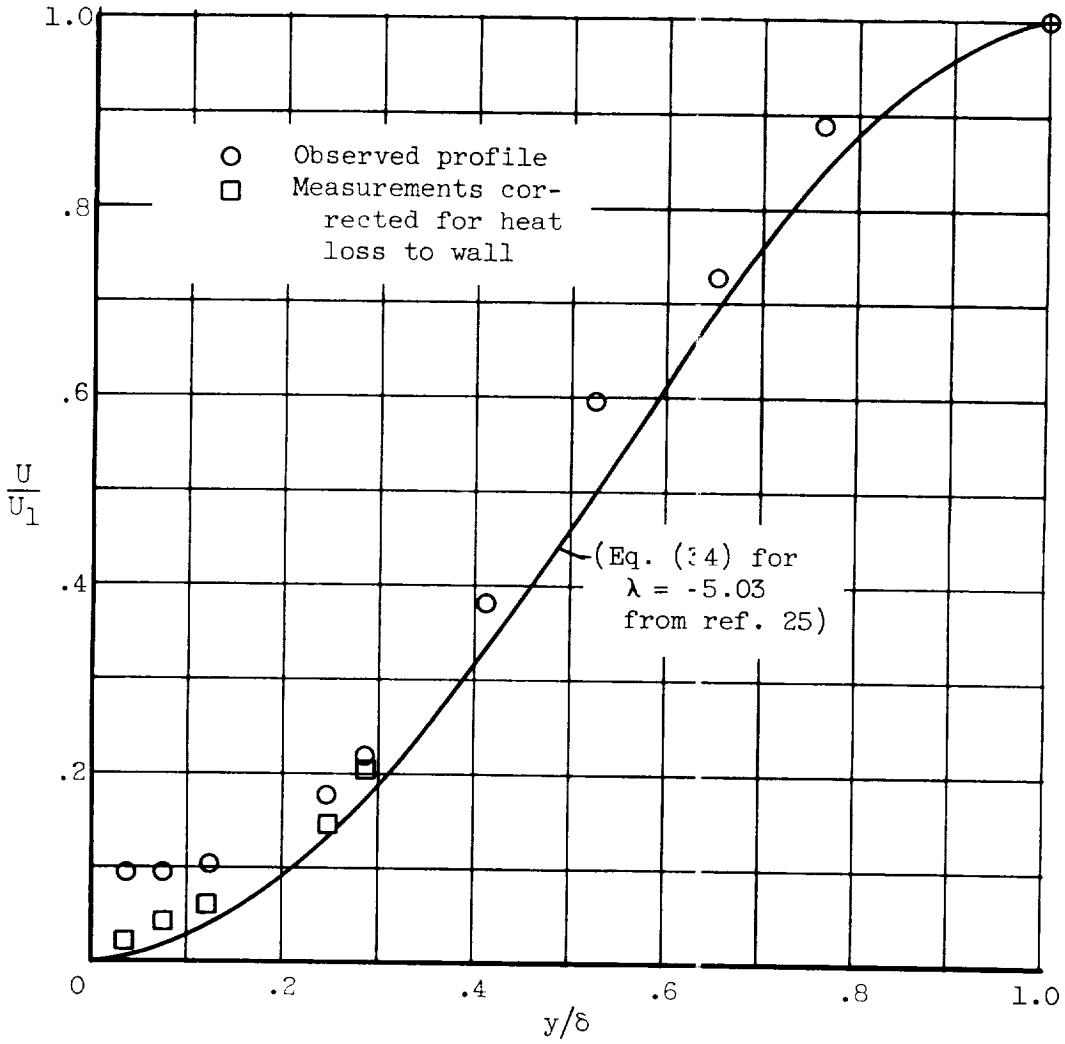

(d) Measurements on an elliptic cylinder (ref. 25); X, 2.029; separation at x = 1.99

Figure 8. - Concluded. Comparison of present equation for laminar separation with various profiles.

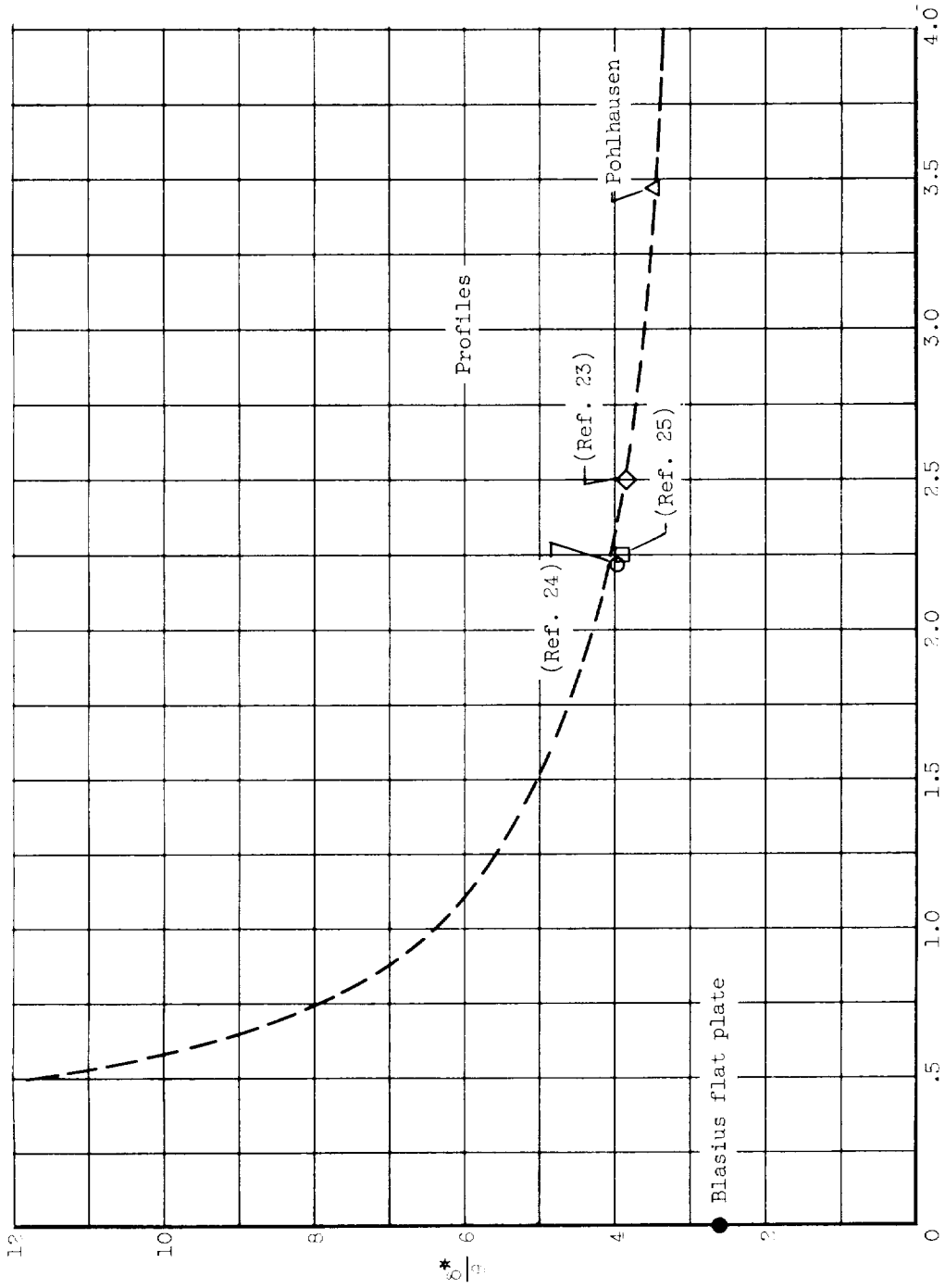

Figure 9. - Relation between δ^*/θ and $\sqrt{-\lambda}$ predicted at laminar separation.